Glioblastoma Stem Cells Generate Vascular Pericytes to Support Vessel Function and Tumor Growth

Lin Cheng,^{1,7} Zhi Huang,^{1,7} Wenchao Zhou,¹ Qiulian Wu,¹ Shannon Donnola,¹ James K. Liu,² Xiaoguang Fang,¹ Andrew E. Sloan,³ Yubin Mao,⁴ Justin D. Lathia,¹ Wang Min,⁵ Roger E. McLendon,⁶ Jeremy N. Rich,¹ and Shideng Bao^{1,*}

¹Department of Stem Cell Biology and Regenerative Medicine, Lerner Research Institute

²Department of Neurosurgery

Cleveland Clinic, Cleveland, OH 44195, USA

³Brain Tumor and Neuro-Oncology Center, University Hospitals, Case Western Reserve University, Cleveland, OH 44106, USA

⁴Department of Pathology, Medical College of Xiamen University, Xiamen, Fujian 361005, China

⁵Department of Pathology, Yale University School of Medicine, New Haven, CT 06520, USA

⁶Department of Pathology, Duke University Medical Center, Durham, NC 27710, USA

⁷These authors contributed equally to this work

*Correspondence: baos@ccf.org

http://dx.doi.org/10.1016/j.cell.2013.02.021

SUMMARY

Glioblastomas (GBMs) are highly vascular and lethal brain tumors that display cellular hierarchies containing self-renewing tumorigenic glioma stem cells (GSCs). Because GSCs often reside in perivascular niches and may undergo mesenchymal differentiation, we interrogated GSC potential to generate vascular pericytes. Here, we show that GSCs give rise to pericytes to support vessel function and tumor growth. In vivo cell lineage tracing with constitutive and lineage-specific fluorescent reporters demonstrated that GSCs generate the majority of vascular pericytes. Selective elimination of GSC-derived pericytes disrupts the neovasculature and potently inhibits tumor growth. Analysis of human GBM specimens showed that most pericytes are derived from neoplastic cells. GSCs are recruited toward endothelial cells via the SDF-1/CXCR4 axis and are induced to become pericytes predominantly by transforming growth factor β. Thus, GSCs contribute to vascular pericytes that may actively remodel perivascular niches. Therapeutic targeting of GSC-derived pericytes may effectively block tumor progression and improve antiangiogenic therapy.

INTRODUCTION

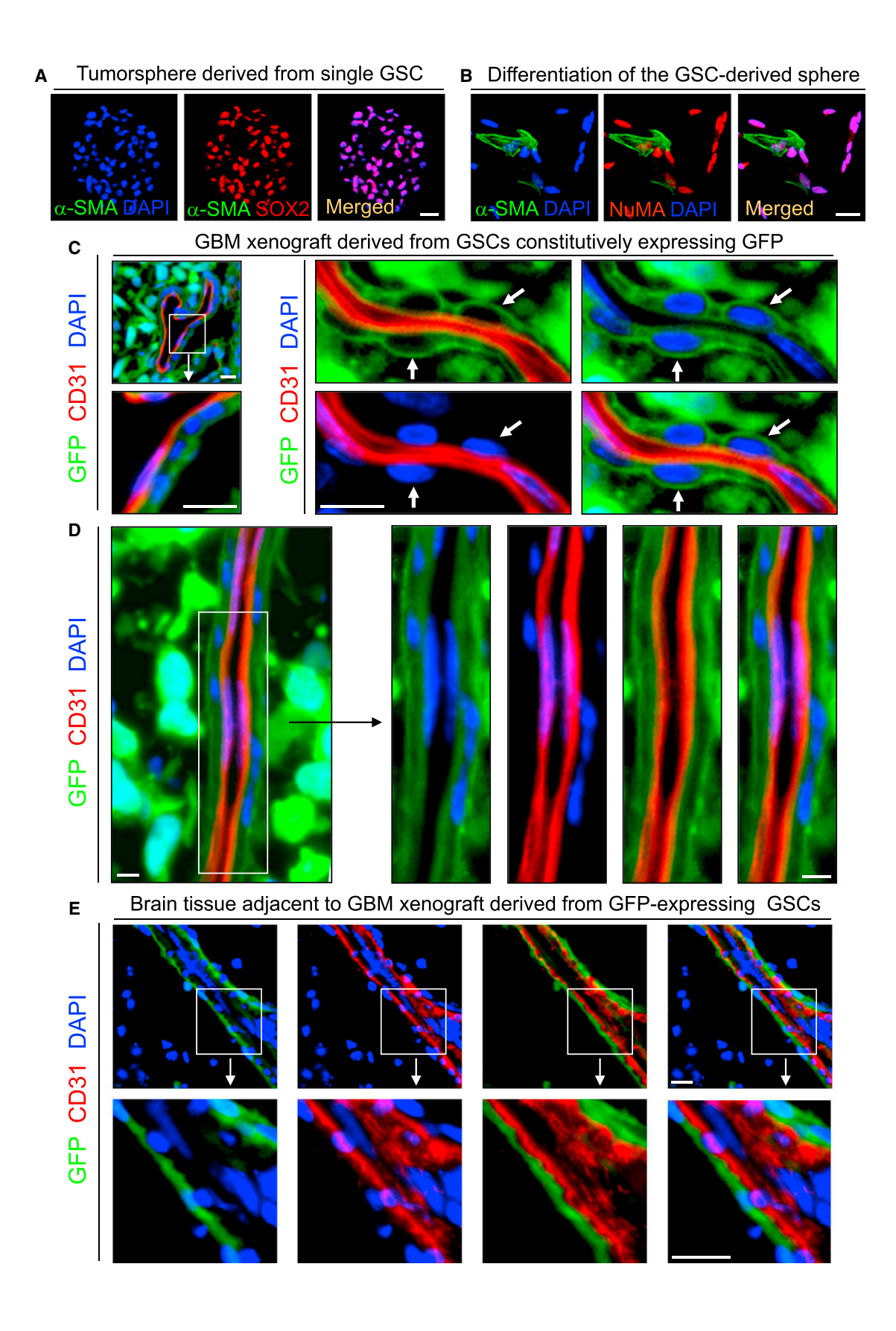
Glioblastomas (GBMs) are fatal tumors with florid vascularization that correlates with tumor malignancy and clinical prognosis (Norden et al., 2009). Targeting endothelial cells (ECs) has been a major focus of antiangiogenic therapeutics, although tumor vessels consist of two distinct but interdependent cellular compartments: ECs and pericytes (Bergers and Song, 2005;

Carmeliet and Jain, 2011). However, most current therapies targeting ECs are not curative and may transform tumor growth pattern toward a more invasive phenotype in GBMs (Pàez-Ribes et al., 2009), suggesting that targeting ECs alone is not sufficient for effective tumor control. Therefore, further insights into tumor vascular development and maintenance have direct translational implications.

Vascular pericytes play critical roles in various physiological contexts, including support of vascular structure and function, maintenance of blood-brain barrier, facilitation of vessel maturation, and initiation of vessel sprouting (Armulik et al., 2010; Bell et al., 2010; Bergers and Song, 2005; Winkler et al., 2011). Pericytes and ECs communicate with each other by direct physical contact and reciprocal paracrine signaling to maintain vessel integrity and function (Franco et al., 2011; Carmeliet and Jain, 2011; Song et al., 2005). Altered association between pericytes and ECs has been shown in tumor vessels (Carmeliet and Jain, 2011; Winkler et al., 2011). Tumor vessels with less pericyte coverage appear more vulnerable to radiation and chemotherapy, suggesting that pericytes are critical to protect ECs and may promote therapeutic resistance (Bergers et al., 2003; Franco et al., 2011). When therapies target ECs in tumors, the pericyte network often maintains a functional core of pre-existing blood vessels (Carmeliet and Jain, 2011). The tumor vasculature frequently exhibits structural and functional abnormality with irregular pericytes on endothelial tubules. The pericyte-EC interaction also differs substantially between tumors and normal tissues (Morikawa et al., 2002; Winkler et al., 2011). However, the mechanisms underlying the abnormality and difference are poorly understood. To better understand the vascular development and maintenance in tumors and lay the foundation for improved targeting therapy, it is essential to determine the interplay between cancer cells and vascular compartments.

GBMs display remarkable cellular hierarchies with tumorigenic glioma stem cells (GSCs) at the apex (Bao et al., 2006a; Calabrese et al., 2007; Zhou et al., 2009), although the cancer





stem cell (CSC) model remains controversial for some tumor types (Magee et al., 2012). We previously demonstrated that GSCs promote tumor angiogenesis through elevated expression of vascular endothelial growth factor (VEGF) (Bao et al., 2006b). This study has been extended by others (Ehtesham et al., 2009; Folkins et al., 2009). GSCs are often located in perivascular niches and interact with ECs in a bidirectional manner (Bao et al., 2006b; Calabrese et al., 2007). Within this context, there was an excitement generated by reports suggesting that GSCs may transdifferentiate into ECs (Ricci-Vitiani et al., 2010; Soda et al., 2011; Wang et al., 2010). These reports have been controversial because the frequency of GSC-EC conversion was not defined, and ECs do not contain cancer genetic alterations in human GBMs (Kulla et al., 2003; Rodriguez et al., 2012). Because pericytes are physically proximal to ECs on vessels, distinguishing ECs and pericytes by location alone poses a challenge. A complementary or competing hypothesis would be a lineage commitment of GSCs to vascular pericytes. There are important reasons to consider GSCs as potential pericyte progenitors. GSCs have the ability to undergo mesenchymal differentiation (deCarvalho et al., 2010; Ricci-Vitiani et al., 2008). GSCs share properties with neural stem cells (NSCs) that display the potential to transdifferentiate into pericytes (li et al., 2009; Morishita et al., 2007). Further, pericytes are similar to mesenchymal stem cells (MSCs) (Crisan et al., 2008). Thus, we investigated the potential of GSCs to generate vascular pericytes and contribute to the remodeling of perivascular niches and determined the significance of GSC-derived pericytes (G-pericytes) in maintaining functional vessels to support GBM tumor growth.

RESULTS

GSCs Are Able to Assume a Pericyte Lineage In Vitro

To investigate a potential lineage link between GSCs and pericytes, we initially examined the capacity of GSCs to differentiate into pericytes in vitro. GSCs were isolated from GBM tumors and validated through functional assays (self-renewal, multipotency, and tumor formation) as previously described (Bao et al., 2006a; Guryanova et al., 2011). Immunofluorescent (IF) staining of freshly sorted GSCs from primary GBMs and the GSC-generated tumorspheres demonstrated SOX2 expression but complete absence of the pericyte markers α smooth muscle actin (α-SMA) and NG2 (Figures S1A and S1B available online), supporting a lack of contamination of GSC populations by pericytes. After GSCs or tumorspheres were induced for differentiation, the differentiated cells contained a fraction (4%-11%) of cells expressing multiple pericyte markers (α-SMA, NG2, CD248, and CD146) (Figures S1C-S1E). To further determine GSC ability to assume a pericyte lineage, we examined the cellular fate of single GSC-derived tumorsphere that did not contain any cell expressing pericyte markers (Figure 1A). Upon differentiation, cells derived from the single GSC-derived tumorsphere contained a fraction of cells expressing pericyte markers (Figure 1B). To rule out potential contamination of host-derived pericyte progenitors in xenograft-derived GSCs, we performed secondary sorting of enriched GSCs with positive selection for the human cell-specific surface antigen TRA-1-85 and negative selection for the pericyte marker CD146. We confirmed that the single GSC-generated spheres derived from the resorted GSCs (SOX2+) did not contain any cell expressing pericyte markers (Figure S1F), whereas differentiated cells derived from the single GSC-derived sphere contained pericyte-marker-expressing cells (Figure S1G). These pericyte-marker-positive cells also expressed the human-cell-specific nuclear antigen NuMA (Figure S1G), confirming that these pericytes were derived from human GSCs, but not from murine pericytes or their progenitors. Collectively, these data demonstrate that GSCs have the capacity to assume a pericyte lineage in vitro.

GSCs Give Rise to Vascular Pericytes in GBM Xenografts In Vivo

To extend the lineage analysis of GSCs in vivo, we examined the origin of pericytes in GBM xenografts and found that pericytes (CD146+CD248+; 2.63%-6.14% of total cells) sorted from the xenografts were largely positive for human NuMA and TRA-1-85 (Figures S1H, S1I, and S1L). In contrast, purified ECs (CD31+CD105+) from GBM xenografts were completely negative for human NuMA and TRA-1-85 (Figures S1J-S1L). We then performed a lineage tracing study by transducing GSCs with GFP constitutive expression and implanted the GSCs orthotopically to establish xenografts. Tumor sections of the xenografts derived from the green fluorescent protein (GFP)-labeled GSCs were immunostained for an EC marker (CD31) and several pericyte markers (α-SMA, Desmin, NG2, CD146, CD248, Ang1, CD13, and platelet-derived growth factor receptor β [PDGFRβ]) because these pericyte markers are expressed in normal brain and primary GBMs (Figures S2A-S2C). No tumor showed GFP-positive ECs, but most tumor vessels were adorned with GFP-positive cells with typical pericytic location and morphology on the vascular external surface (Figures 1C and 1D). IF analyses of pericyte markers further confirmed that expression of pericyte markers (Desmin, α-SMA, NG2, PDGFRβ, CD248, and CD146) overlapped with GFP in the majority (mean 78%, range 57%-89%) of pericytes (Figures 2A and 2B; Figures S2D and S2E), indicating that the majority of vascular pericytes were derived from GSCs. We validated this result in 21 GBM xenografts using GFP-labeled GSCs isolated from 12 primary GBMs and 9 GBM xenografts, suggesting that the contribution of GSCs to pericytes is a common event during

Figure 1. GSCs Have the Potential to Assume a Pericyte Lineage

(A) IF staining of SOX2 (a GSC marker) and α -SMA (a pericyte marker) in the single GSC-derived tumorsphere. Nuclei were stained with DAPI. (B) IF staining of α -SMA and NuMA (a human cell-specific nuclear antigen) in differentiated cells derived from the single GSC-derived tumorsphere. (C and D) In vivo lineage tracing of GSCs with GFP constitutive expression. Sections of GBM tumors derived from the GFP-labeled GSCs (D456 or CCF2170) were immunostained for CD31 to mark ECs and counterstained with DAPI. Arrows indicate GFP+ cells with pericytic location. (E) IF staining of CD31 in peritumoral brain adjacent to the GBM tumor derived from GFP-labeled GSCs (CCF2170). All scale bars represent 25 μ m. See also Figure S1.

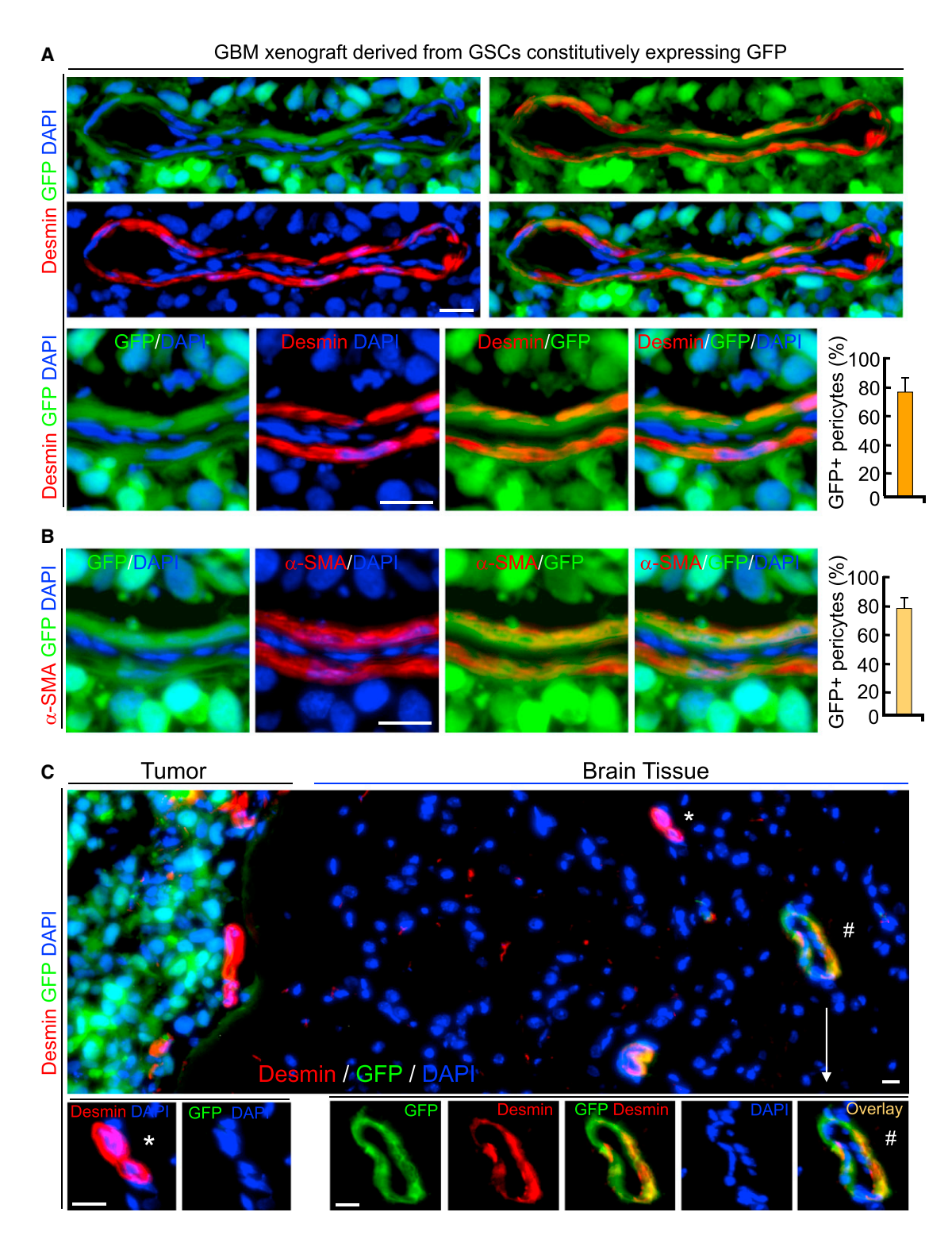


Figure 2. GSCs Generate Pericytes Expressing Specific Markers In Vivo

(A and B) In vivo lineage tracing of GSCs and IF staining of pericyte marker Desmin (A) or α -SMA (B) in GBM tumors derived from GFP-labeled GSCs (D456). Quantifications show fractions of G-pericytes (GFP⁺ and Desmin⁺/ α -SMA⁺).

(C) IF staining of Desmin in peritumoral brain adjacent to GBM tumor derived from GFP-labeled GSCs (CCF1468). A vessel containing G-pericytes (Desmin⁺ and GFP⁺) in peritumoral brain was marked (#) and enlarged.

All scale bars represent 20 $\mu\text{m}.$ The error bars represent SD. See also Figure S2.

GBM growth. Notably, a minor fraction (mean 22%, range 11%–43%) of vascular pericytes in the GBM xenografts did not overlap with GFP expression, indicating that these pericytes were host derived. Most tumor vessels had a mixture of GSC- and host-derived pericytes (Figure 2A). Taken together, these data demonstrate that GSCs have the capacity to generate the majority of vascular pericytes in GBM xenografts.

Peritumoral Brain Vessels Contain G-Pericytes

Because GBMs commonly invade into normal brain, we examined whether GSCs contribute to vascular pericytes in peritumoral brain. We found that a subset of vessels in peritumoral brain adjacent to the GFP-labeled GSC xenograft also contain GFP-positive pericytes (Figure 1E). IF analyses validated a fraction of vessels coexpressing pericyte markers and GFP and in brain tissue near the GFP tumor (Figure 2C). These data indicate that GSCs can also give rise to pericytes in the peritumoral brain. Notably, G-pericytes (GFP+) were detectable not only in peritumoral brain but also in tumor-free brain up to 0.86 mm distant from the tumor edge, suggesting that GSCs were recruited by ECs in the peritumoral brain to generate pericytes. Thus, GSCs also generate vascular pericytes in the peritumoral brain.

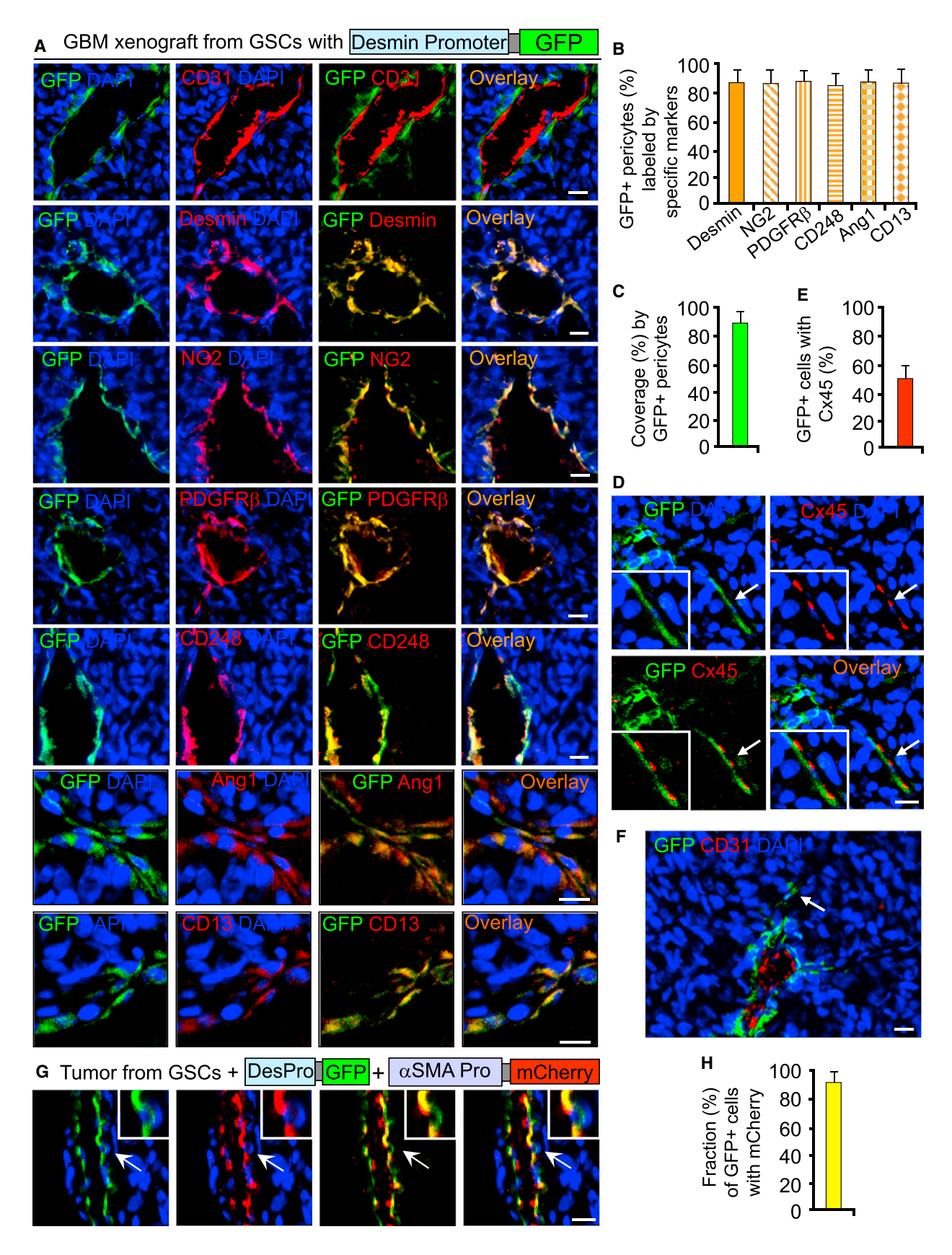
Validation of G-Pericytes by Lineage-Specific Fluorescent Reporters

To provide direct evidence validating GSC capacity to generate pericytes in vivo, we performed in vivo cell lineage tracing of GSCs with a pericyte marker (Desmin or α-SMA) promoterdriven expression of GFP or mCherry, which served as fluorescent reporters of pericyte lineage. We cloned the human Desmin promoter (Li and Paulin, 1991) and α -SMA core promoter (Keogh et al., 1999; Nakano et al., 1991) and then generated lentiviral constructs for the Desmin promoter-driven GFP expression (DesPro-GFP) or α -SMA promoter-driven mCherry expression (aSMAPro-mCherry). We confirmed that the cloned Desmin and α -SMA promoters were functional and pericyte specific because GFP or mCherry expression occurred specifically in human brain vascular pericytes (HBVPs) (Figure S3A, left). We then implanted DesPro-GFPtransduced GSCs into mouse brains and examined tumor vessels by IF analysis. DesPro-driven GFP expression specifically marked perivascular cells that expressed pericyte markers, including Desmin, NG2, PDGFRβ, CD248, Ang1, and CD13 (Figures 3A-3C), validating that GSCs generated vascular pericytes in the GBM xenografts. The G-pericytes also expressed the gap junction protein connexin45 (Cx45) that is often localized at pericyte-EC contacts (Figures 3D and 3E). Notably, GFP-positive cells were mainly located in perivascular regions close to vessels but rarely detected in regions distant from vessels in tumors (Figure 3F). We further performed an additional pericyte lineage tracing of GSCs cotransduced with DesPro-GFP and αSMAPro-mCherry and detected coexpression of mCherry and GFP in perivascular cells (Figures 3G and 3H). GFP+ perivascular cells were abundant around vessels and the majority of pericyte-marker-positive cells (>83%) expressed GFP (Figures 3A-3F), confirming that GSCs generated the majority of pericytes in these tumors.

Tumor pericytes often exhibit abnormal morphologies, sometimes extending their processes away from the endothelium (Morikawa et al., 2002). The G-pericytes often displayed such irregular morphology (Figures 3A and 3F). Recent appreciation of intertumoral heterogeneity of GBMs has informed a mesenchymal subtype in contrast to proneural and classical subtypes (Verhaak et al., 2010). Interestingly, in vivo lineage tracing showed that mesenchymal GSCs have significantly greater ability to generate pericytes than classic and proneural GSCs in xenografts (Figures S3B and S3C; Table S1). Collectively, these data provide direct evidence demonstrating that GSCs have the capacity to generate pericytes in vivo.

Because our in vivo cell fate tracing of GSCs with GFP constitutive expression failed to detect GSC-derived ECs (Figures 1C and 1D), we performed the cell lineage tracing of GSCs with an EC marker (CD31 or CD105) promoter-driven GFP expression to directly address whether GSCs generate ECs. We cloned the human CD105 (endoglin) promoter (Ríus et al., 1998) and the CD31 (PECAM-1) promoter restricted to ECs (Almendro et al., 1996; Gumina et al., 1997) and then generated lentiviral constructs for conditional GFP expression driven by CD31 or CD105 promoter (CD31Pro-GFP or CD105Pro-GFP). We validated that the cloned CD31 and CD105 promoters were functional and EC specific because CD31Pro- or CD105Pro-driven GFP expression specifically occurred in ECs (human brain microvessel endothelial cells [HBMECs]) (Figure S3A, right), To perform EC lineage tracing of GSCs, GSCs with CD31Pro-GFP or CD105Pro-GFP were orthotopically implanted into mouse brains. In confirmation with our earlier studies, no GFP expression was detectable in tumor ECs marked by CD31 and Glut1 staining (Figures S3D and S3E), further ruling out the possibility of GSC-derived ECs in GBM xenografts.

To further characterize the G-pericytes, we examined pericyte marker expression in G-pericytes and HBVP pericytes. We isolated G-pericytes by sorting GFP+CD146+ cells from GBM xenografts derived from the DesPro-GFP-GSCs. Comparative RT-PCR analyses of key pericyte markers (α-SMA, Desmin, CD248, NG2, CD146, and PDGFRβ) in the sorted G-pericytes and HBVPs confirmed similar marker expression in the GBM xenografts (Figure S4A). To address whether G-pericytes still express GSC markers after lineage switching, we examined expression of several putative GSC markers (SOX2, OLIG2, CD133, and Nestin) and pericyte markers in sorted GSCs (CD15+L1CAM+) and G-pericytes (GFP+CD146+). RT-PCR analyses showed that G-pericytes no longer express the GSC markers (Figure S4B). This result was confirmed by IF staining of SOX2, OLIG2, or Nestin on frozen sections of the DesPro-GFP-GSC xenografts. Consistently, GFP expression was turned on specifically in perivascular cells that rarely (<0.8%) expressed SOX2, OLIG2, or Nestin (Figure S4C, S4D, and S4F). In contrast, the SOX2, OLIG2, or Nestin-expressing cells (GSCs) are localized near perivascular niches (Figure S4C and S4D). The mutually exclusive expression of GSC and pericyte markers suggests that GSCs undergo differentiation to generate G-pericytes rather than being a GSC subpopulation adjacent to ECs in GBM tumors. In addition, G-pericytes do not express astrocyte markers such as glial fibrillary acidic protein (GFAP) and S100ß (Figures S4A, S4E, and S4F), indicating that G-pericytes are



not a subpopulation of astrocytes. Consistently, pericytes and astrocytes are distinct cell populations without overlapping expression of specific markers in primary GBMs (Figure S4G). These data demonstrate that G-pericytes are unique cells expressing specific pericyte markers.

Pericytes in Primary GBMs Are Commonly Derived from Neoplastic Cells

To examine whether pericytes are lineage related to cancer cells in human primary GBMs, we performed fluorescence in situ hybridization (FISH) analyses of common GBM genetic changes (Cancer Genome Atlas Research Network, 2008) in combination with IF staining of a pericyte marker (α -SMA) to determine if pericytes carry cancer genetic alterations in GBMs. Because gains of chromosome 7 (EGFR amplification) or losses of chromosome 10 (PTEN loss) are frequent in GBM cells, permitting a lineage tracing to the neoplastic cells, we employed DNA probes for centromeres of chromosome 7 (CEP-7) and 10 (CEP-10), EGFR, and PTEN to detect cancer genetic alterations in pericytes, ECs, and tumor cells in GBM tissue microarrays. FISH analyses showed the majority of tumor pericytes (mean 76%, range 58%-83%) carried the same genetic alterations (CEP-7 polysomy, EGFR trisomy or amplification, CEP-10 loss, or PTEN loss) as cancer cells in 49 GBMs (Figures 4A and 4B), indicating that tumor pericytes are commonly derived from cancer cells. In contrast, we rarely detected relevant genetic changes in ECs in these GBMs (Figures S5A and S5B). To further confirm these results, we isolated pericytes (CD146+CD248+; 2.18%-5.26% of total cells) and ECs (CD31+CD105+) from primary GBMs and performed similar FISH analyses. The majority (>72%) of sorted tumor pericytes (α-SMA+) carried the same genetic alteration (CEP-7 polysomy) as matched GSCs (Figures 4C and 4D). In contrast, sorted ECs (CD31+CD105+) expressed Glut1 but did not share the GSC genetic alterations (Figure S5C and S5D). These results support a tumor source for pericytes, but not for ECs in human primary GBMs.

To further address whether pericytes in endogenous GBMs are derived from cancer cells, we examined pericytes in the genetically engineered mouse GBMs (Nestin-tva/Ink4a/Arf^{-/-}/ HA-PDGFB models; Hambardzumyan et al., 2009). IF staining of hemagglutinin-tagged platelet-derived growth factor B (HA-PDGFB) and pericyte markers (Desmin, NG2, CD248, or α -SMA) showed that a significant fraction (mean 63%) of tumor pericytes expressed HA-PDGFB, supporting a tumor origin (Figure 4E, 4F; data not shown). In contrast, staining of EC markers (CD31 or Glut1) and HA-PDGFB showed no tumor-cell-derived ECs in these mouse GBMs (Figure S5E). These data demonstrate that pericytes in the genetically engineered mouse GBMs are also largely derived from neoplastic cells.

Selective Elimination of G-Pericytes Disrupts Tumor Vessels and Inhibits Tumor Growth

To determine the functional significance of G-pericytes, we examined effects of selective elimination of G-pericytes on vessels and tumor growth. GSCs were transduced with Desmin-promoter-driven expression of herpes simplex virus thymidine kinase (HsvTK) (Figure 5A) to achieve conditional HsvTK expression in G-pericytes. Because HsvTK metabolizes ganciclovir (GCV) into a toxic agent specifically in cells expressing HsvTK (Culver et al., 1992), G-pericytes expressing HsvTK should be sensitive to GCV and thus eliminated by GCV treatment. To confirm selective killing of G-pericytes expressing Desmin-promoter-driven HsvTK by GCV treatment, we generated a construct for coexpression of HsvTK and GFP under the same promoter (DesPro-TK-GFP) (Figures 5A and S6A). As expected, after the DesPro-TK-GFP-transduced GSCs were induced to differentiate, GFP was expressed in a fraction of differentiated cells (G-pericytes) (Figure S6B). Apoptotic detection showed that GCV treatment selectively induced apoptosis in cells coexpressing GFP and HsvTK (Figure S6C). These data indicate that selective elimination of G-pericytes is achievable by using Desmin-promoter-driven HsvTK conditional expression with GCV treatment.

To examine the impact of selective targeting of G-pericytes on tumor vessels, we implanted DesPro-TK-GFP-GSCs into mouse brains. Mice bearing the tumors were treated with vehicle control or GCV daily to induce HsvTK-mediated toxicity to G-pericytes. Apoptotic detection by TUNEL staining demonstrated that GCV treatment for 3 days selectively induced cell death in G-pericytes (GFP+) in vivo (Figure 5B). Further, GCV treatment for 1 week caused almost a complete depletion of G-pericytes, collapse of vessel lumens, and disruption of endothelial walls in GBM tumors (Figures 5C, 5D, S6D and S6E). Moreover, measurement of vascular function by fluorescein isothiocyanate (FITC)-conjugated mega-dextran showed that GCV treatment for 1 week to deplete G-pericytes severely attenuated vascular function in the DesPro-TK-GSC xenografts, because perfusion of FITCmega-dextran into the tumors was dramatically reduced (Figures 5E, 5F, S6F and S6G). Collectively, these data demonstrate that selective elimination of G-pericytes potently disrupts vascular structure and function in GBM tumors.

To evaluate the impact of selective targeting of G-pericytes on tumor growth, we initially used subcutaneous tumor experiments to track sequential tumor volumes. The established subcutaneous tumors derived from the DesPro-TK-GFP-GSCs were treated with GCV or vehicle control for 3 weeks. GCV treatment caused significant regression of the tumors (Figures 5G and 5H), indicating that selective elimination of G-pericytes by HsvTKinduced GCV toxicity inhibited tumor growth. To further validate

Figure 3. In Vivo Lineage Tracing of GSCs with Pericyte-Specific Promoter-Driven Fluorescent Reporters

(A-F) In vivo lineage tracing of GSCs with Desmin promoter-driven GFP (DesPro-GFP). Sections of GBM tumors derived from DesPro-GFP-GSCs were immunostained for an EC marker (CD31), a pericyte marker (Desmin, NG2, PDGFRB, CD248, Ang1, or CD13) (A), or the pericyte-EC junction marker Cx45 (D). Quantifications show fractions of GFP+ pericytes (B), coverage by GFP+ pericytes (C), or the fraction of GFP+ pericytes expressing Cx45 (E). An arrow indicates rare GFP+ pericytes away from vessels (F).

(G and H) In vivo lineage tracing of GSCs with coexpression of Desmin promoter-driven GFP and α-SMA promoter-driven mCherry in GBMs. Quantification shows the fraction of GFP+ cells with mCherry.

All scale bars represent 25 µm. The error bars represent SD. See also Figures S3, S4, and Table S1.

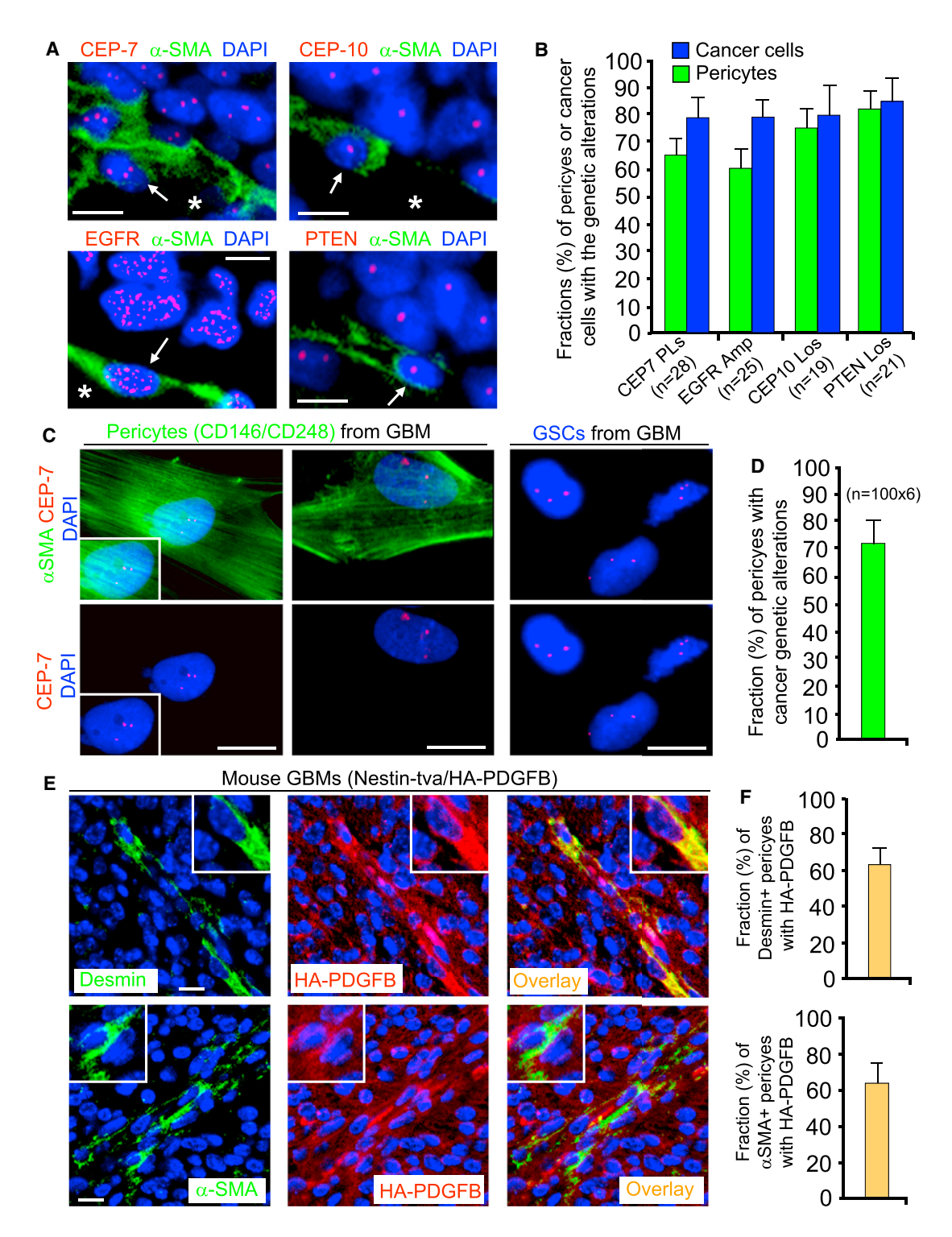


Figure 4. Pericytes Are Commonly Derived from Neoplastic Cells in Primary GBMs

(A and B) FISH analyses of genetic alterations with the CEP-7, CEP-10, EGFR, or PTEN probe (in red) in pericytes (α -SMA⁺) in primary GBMs. Quantification shows average fractions of pericytes carrying the cancer genetic alterations (CEP-7 polysomy, EGFR amplification or trisomy, CEP-10 loss, or PTEN loss) in GBM tissue arrays (B). (C and D) FISH analyses with CEP-7 probe in sorted pericytes (α -SMA⁺) and GSCs from primary GBMs. Quantification shows the fraction (mean 72%) of pericytes carrying the GSC genetic alterations (D).

(E and F) IF staining of a pericyte marker (Desmin or α-SMA) and HA-PDGFB in the genetically engineered mouse GBMs (Nestin-tva/Ink4a/Arf^{-/-}/HA-PDGFB model). Quantifications show fractions (mean 63%) of HA-PDGFB⁺ pericytes (F)

The scale bars represent 10 μm (A and C) and 25 μm (E). The error bars represent SD. See also Figure S5.

this result in orthotopic tumors, we transduced GSCs either with DesPro-GFP (control) or DesPro-TK and implanted these GSCs into mouse brains to establish GBM xenografts. Both groups of mice bearing the tumors were administered with GCV to eliminate the G-pericytes expressing HsvTK. GCV treatment for 2 weeks caused extensive vessel regression in GBM tumors derived from DesPro-TK-GSCs, but not from DesPro-GFP-GSCs (Figures S6H and S6I). Moreover, GCV treatment for 3 weeks markedly inhibited intracranial tumor growth in GBM xenografts derived from DesPro-TK-GSCs, but not in control tumors from DesPro-GFP-GSCs (Figures 5I and 5J). Alternatively, treatment by GCV, but not vehicle control suppressed intracranial tumor growth in the GBM xenografts derived from DesPro-TK-GSCs (Figure S6J). As a consequence, GCV treatment significantly increased survival of animals implanted with the DesPro-TK-GSCs (Figure 5K). These data demonstrate that selective elimination of G-pericytes suppressed GBM tumor growth and malignant progression.

GSCs Are Recruited toward ECs via the SDF-1/CXCR4 Axis

To understand the mechanisms underlying GSC recruitment toward ECs, we examined whether GSCs can be recruited by HBMECs to support the maintenance of EC complexes in vitro. GSCs labeled with the green fluorescent tracer CFSE were mixed with HBMEC complexes labeled with the red fluorescent tracer CMTRX. Integration of GSCs-derived cells into EC complexes was detected on day 2 after cell mixing, and the integration stabilized the EC complexes for extended periods (2.6-fold) relative to EC complex alone (Figure 6A). To address whether pericyte lineage specification of GSCs can be induced by EC complexes, we cocultured GSCs with HBMECs and detected integration of G-pericytes by α -SMA staining (Figure 6B). Because the attachment of pericytes to ECs can be mediated through adherens junctions containing N-cadherin (Gerhardt et al., 2000), we examined N-cadherin expression and found that N-cadherin was localized to the contact sites between G-pericytes (α-SMA+) and EC complexes (Figure 6B).

To define the molecular mechanisms underlying GSC recruitment by ECs, we analyzed the effect of several chemotactic factors (SDF-1 α , PDGFB, and transforming growth factor β [TGF- β]) secreted by HBMECs on GSC migration. We found that SDF-1 potently stimulated GSC migration (Figures S7A and S7B), whereas PDGFB only modestly attracted GSCs. To further address whether HBMECs attract GSCs via SDF-1, we cocultured GSCs and HBMECs in separate chambers of transwells and detected that HBMECs potently attracted GSCs, an effect dependent on SDF-1 because an anti-SDF-1 antibody attenuated the effects (Figures S7C and S7D). Because ECs in brain and GBMs constitutively express SDF-1 (Kokovay et al., 2010; Komatani et al., 2009), we confirmed that abundant SDF-1 formed a gradient around vessels with greater SDF-1 proximal to vessels in brain and GBMs (Figure S7E).

Because SDF-1 is secreted by ECs and GSCs express the SDF-1 receptor CXCR4 (Ehtesham et al., 2009; Folkins et al., 2009), we hypothesized that brain ECs may recruit GSCs at least in part through the SDF-1/CXCR4 axis. CXCR4 knockdown in GSCs reduced the recruitment of GFP-labeled GSCs to EC

complexes (Figures 6C and 6D). In addition, an SDF-1 blocking antibody significantly reduced the integration of GFP-labeled GSCs into HBMEC complexes (Figures S7F and S7G). As a further confirmation, we examined the effect of a CXCR4 inhibitor (AMD3100) on GSC recruitment to EC complexes. AMD3100 treatment significantly reduced the integration of GSCs (CMTRX labeled, in red) into CFSE-labeled HBMECs (in green) (Figures S7H and S7I).

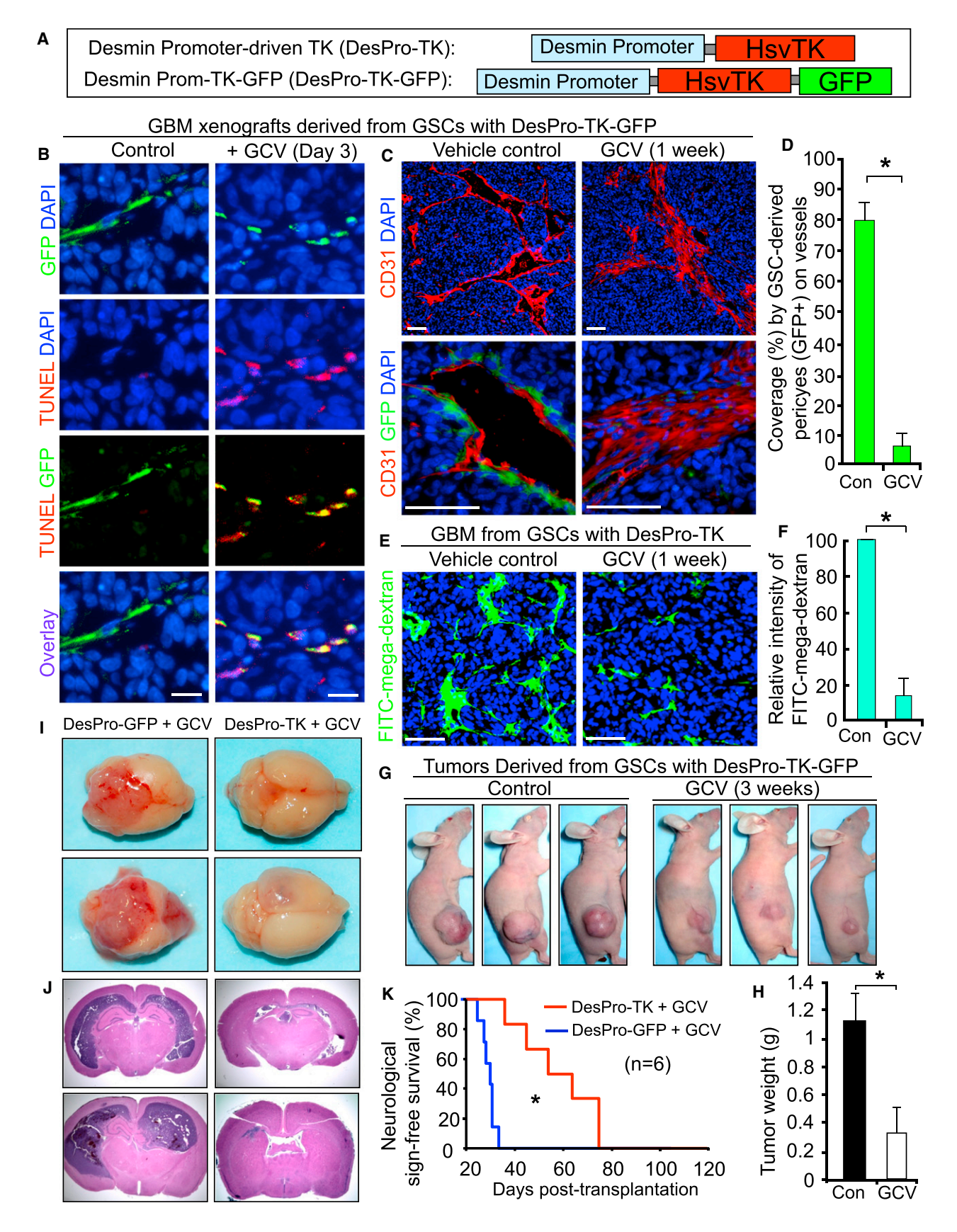
To further determine whether GSC recruitment to ECs depends on the SDF-1/CXCR4 axis during tumor vascularization, GFP-labeled GSCs were transduced with shCXCR4 or nontargeting small hairpin RNA (shNT) and implanted into mouse brains. In shNT xenografts, tumor vessels were covered with abundant G-pericytes (GFP+ and Desmin+), whereas G-pericytes and total pericyte coverage on vessels was significantly reduced in shCXCR4 xenografts (Figures 6E-6G). Immunohistochemical (IHC) staining confirmed that CXCR4 knockdown significantly decreased vessel density in the tumors (Figures S7J and S7K). Collectively, these data suggest that ECs recruit GSCs via the SDF-1/CXCR4 axis and that targeting this pathway reduces G-pericytes in GBMs.

TGF- β Induces Differentiation of GSCs into Pericytes

We next sought to understand the molecular mechanisms underlying the pericyte lineage specification of GSCs. To identify the potential factors inducing GSC differentiation into pericytes. we examined the effect of several EC-secreted cytokines (SDF-1, PDGFB, and TGF-β) on GSC differentiation into pericytes. Immunoblot analysis showed that TGF-β dominantly induced expression of α-SMA when GSCs were cultured in differentiation media (Figures 7A and 7B). IF staining of multiple pericyte markers (NG2, α-SMA, CD146 and CD248) confirmed that TGF-β treatment increased the fraction of cells expressing pericyte markers in the differentiated cells (Figures 7C and 7D; data not shown). Further, TGF- β treatment induced GFPexpressing cells in differentiated cells derived from DesPro-GFP-GSCs (Figures 7E and 7F). To address whether ECs induce GSC differentiation into pericytes through TGF- β , we cocultured DesPro-GFP-GSCs and HBMEC complexes and monitored GFP-expressing cells (G-pericytes) over time. GFP+ cells were induced and integrated into EC complexes, an effect that was attenuated by incubation of the EC complexes with an anti-TGF-β antibody (Figure 7G). Immunoblot analysis validated that coculture of GSCs with HBMECs or their conditioned media induced expression of pericyte marker α-SMA in differentiated cells, an effect that was reduced by a TGF-\$\beta\$ neutralizing antibody (Figure 7H). Collectively, these data demonstrate that HBMECs induce pericyte lineage specification of GSCs at least in part through TGF-β. Thus, the recruitment of GSCs toward ECs via the SDF-1/CXCR4 axis and the induction of GSC differentiation into pericytes by TGF-β are two events controlled by different molecular mechanisms (Figure 7I).

DISCUSSION

Pericytes play essential roles to maintain functional vessels to support tumor growth. Tumor pericytes are thought to be derived from their progenitors from the surrounding normal



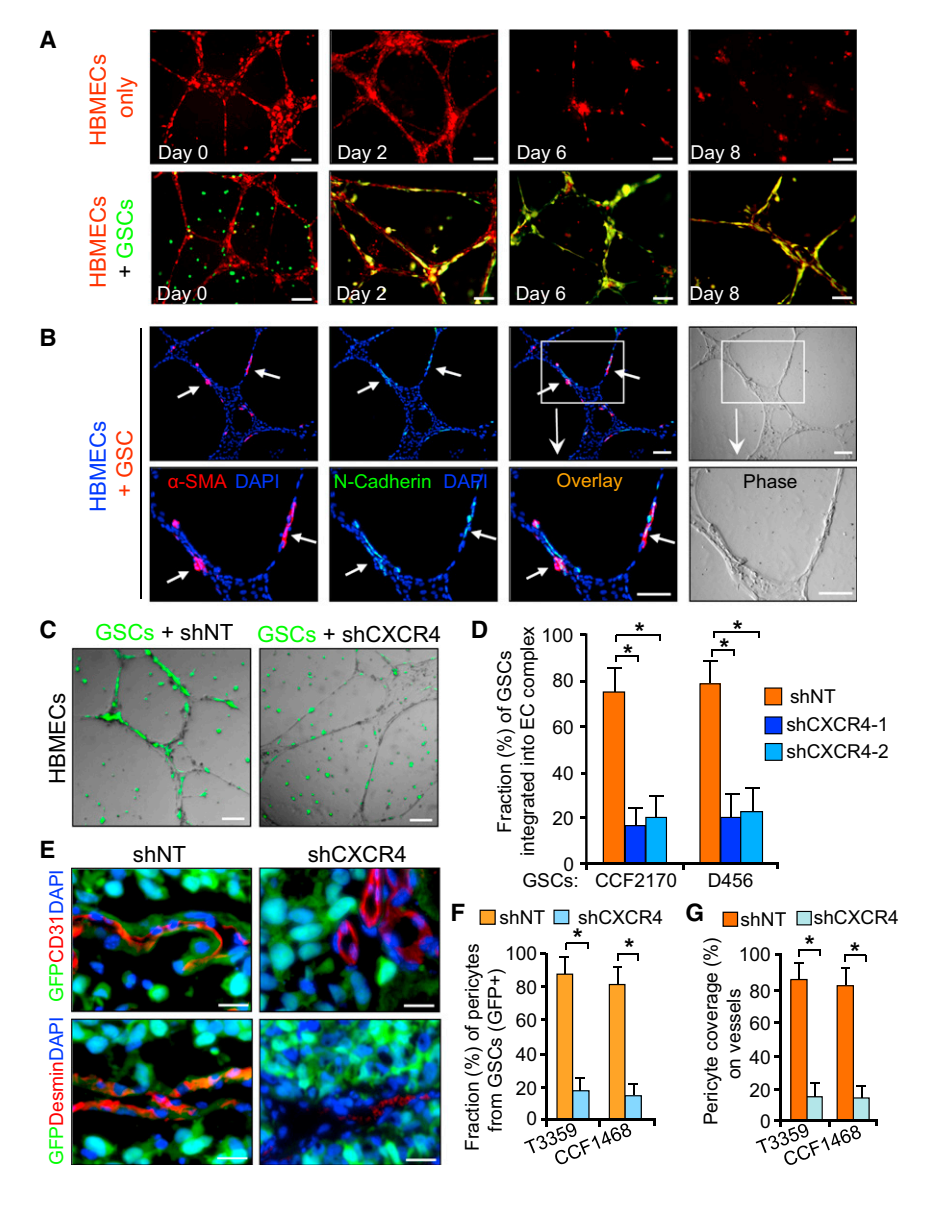


Figure 6. GSCs Are Recruited toward ECs through the SDF-1/CXCR4 Axis to Support **Endothelial Complex**

(A) In vitro endothelial complex formation of HBMECs (labeled with red fluorescent tracer CMTRX) with or without GSCs (labeled with CFSE,

(B) IF staining of α -SMA and N-cadherin in complexes of HBMECs and GSC-derived cells. Nuclei were stained with DAPI.

(C and D) Endothelial complexes of HBMECs with GFP-labeled GSCs expressing shCXCR4 or shNT. Quantification shows fractions of GSC-derived cells (GFP+) on HBMEC complexes (D), *p < 0.001. (E-G) In vivo lineage tracing of GSCs with GFP constitutive expression and IF staining of CD31 or Desmin in tumors derived from GSCs expressing shCXCR4 or shNT. Quantifications show fractions of G-pericytes (GFP+) (F) and total pericyte coverage (G) on vessels. *p < 0.001.

The scale bars represent 100 µm (A-C) and 25 μm (E). The error bars represent SD. See also Figure S7.

in GBMs are derived from GSCs. Because G-pericytes express similar pericyte markers as normal brain vascular pericytes, GSCs function as pericyte progenitors and contribute to vasculature formation in GBMs. The ability of GSCs to generate vascular pericytes in vivo suggests that GSCs may actively remodel their microenvironment and create a supportive niche, permitting functional vessels to augment tumor growth without depending on the limited source of normal pericyte progenitors surrounding tissues.

Because NSCs can transdifferentiate into pericytes (li et al., 2009; Morishita et al., 2007), a lineage link between

NSCs and pericytes is present in normal tissues. Because GSCs share regulatory programs with NSCs, the plasticity of GSCs toward a pericyte lineage may be a product of aberrant

tissue or from the bone-marrow-derived cells homing in tumors after treatments (De Palma et al., 2005; Du et al., 2008). In this study, we demonstrate that the majority of vascular pericytes

Figure 5. Selective Elimination of G-Pericytes Disrupts Tumor Vessels and Inhibits Tumor Growth

(A) Schematic illustrations of Desmin-promoter-driven expression of HsvTK and coexpression of HsvTK and GFP.

(B) TUNEL assay detecting selective apoptosis (in red) of G-pericytes (GFP+) induced by ganciclovir (GCV) in GBM tumors derived from DesPro-TK-GFP-GSCs (CCF2170).

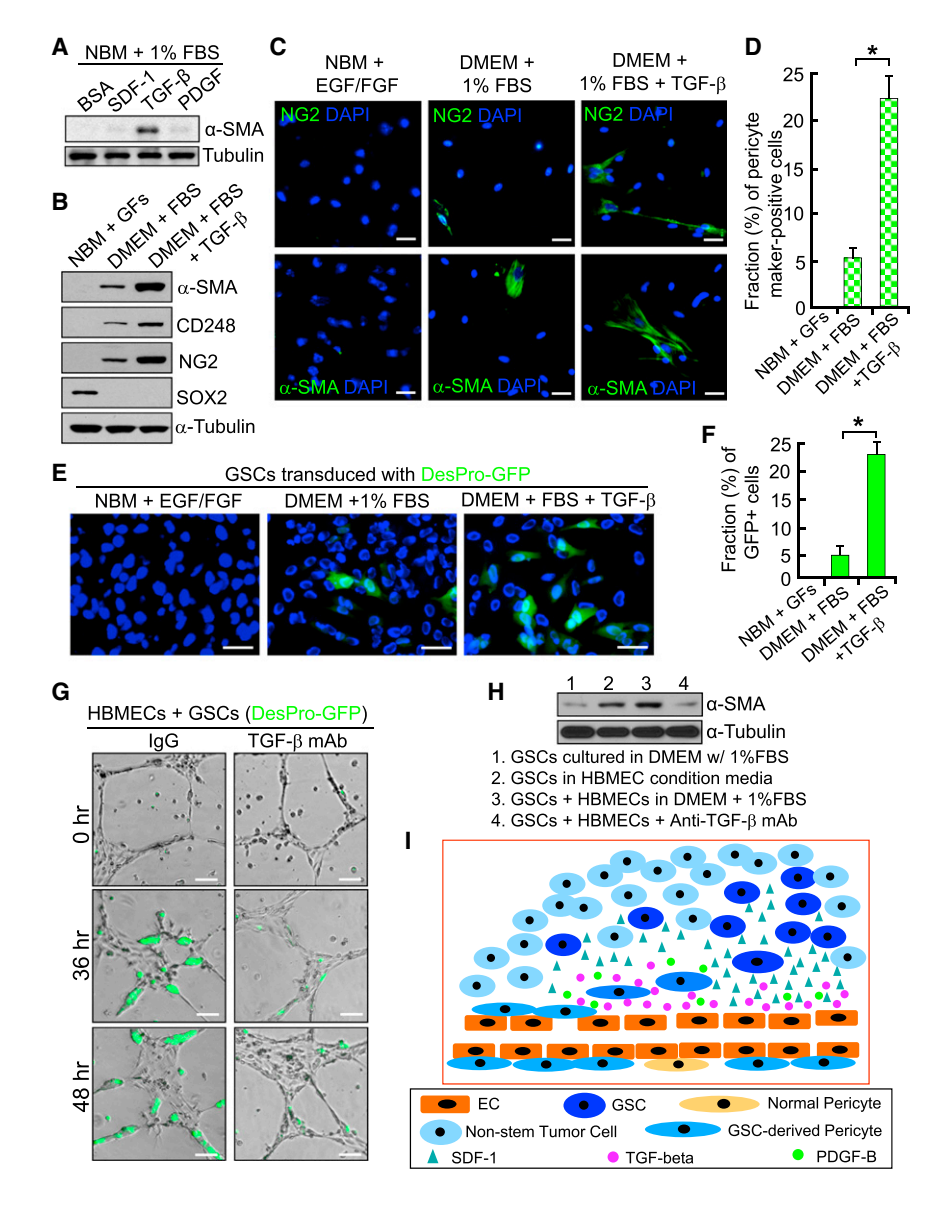
(C and D) IF staining of CD31 (in red) shows effects of selective elimination of G-pericytes (GFP+) by GCV on vessels in GBM tumors derived from DesPro-TK-GFP-GSCs. Quantification shows the reduced G-pericyte coverage by GCV treatment (D). *p < 0.001.

(E and F) Assessment of vascular function using the FITC-conjugated mega-dextran after selective elimination of G-pericytes in GBM tumors derived from DesPro-TK-GSCs. Quantification shows intensity of perfused FITC-mega-dextran into the control or GCV-treated tumors (F). *p < 0.001.

(G and H) The effect of targeting G-pericytes by GCV treatment on growth of subcutaneous tumors derived from DesPro-TK-GFP-GSCs. Quantification shows mean tumor weights in the control and GCV-treated mice (H). p < 0.001 (n = 12).

(I and J) The effect of selective elimination of G-pericytes on GBM growth in mouse brains. Mice bearing tumors derived from DesPro-TK-GSCs or DesPro-GFP-GSCs (control) were treated with GCV for 3 weeks. Images of whole brains (I) and histological analysis (hematoxylin and eosin [H&E] staining) on brain sections (J) are shown.

(K) Kaplan-Meier survival curves of mice bearing GBM tumors derived from DesPro-TK-GSCs or DesPro-GFP-GSCs (control) after GCV treatment. *p < 0.001 (n = 6). The scale bars represent 25 μm (B) and 100 μm (C and E). The error bars represent SD. See also Figure S6.



developmental biology. Although previous reports suggest that GSCs may give rise to ECs in GBMs (Ricci-Vitiani et al., 2010; Soda et al., 2011; Wang et al., 2010), such an event may be very rare because ECs in GBMs rarely carry the cancer genetic mutations as demonstrated in our study and others (Kulla et al., 2003; Rodriguez et al., 2012). Moreover, our complementary lineage tracing studies failed to demonstrate GSC-derived ECs in vivo, although in the culture condition we occasionally observed rare EC-marker-expressing cells (<0.6%) in differentiated cells from GSCs. Because vascular pericytes closely attach to ECs and both cells appear very thin, prior studies may have missed the true identity of tumor-derived cells on vessels. Because both ECs and pericytes express Tie2 (De Palma et al., 2005), the use of Tie2 promoter-driven HsvTK expression for targeting "GSC-derived ECs" (Ricci-Vitiani et al., 2010) might actually eliminate the G-pericytes. Our in vivo lineage tracing with pericyte- or EC-specific promoter-driven fluorescent reporters

Figure 7. TGF- β Induces Differentiation of **GSCs into Pericytes**

(A) Immunoblot (IB) analysis of pericyte marker (α-SMA) expression in differentiated cells from GSCs (CCF1992) in the presence of indicated cytokines (1 ng/ml) in culture media.

(B) IB analysis of pericyte markers (α-SMA, CD248, and NG2) and a GSC marker (SOX2) in GSCs and differentiated cells with or without treatment of TGF-β (2 ng/ml).

(C and D) IF staining of pericyte markers (NG2 and α -SMA) in GSCs (CW1217) and differentiated cells induced by serum or TGF-β. Quantification shows pericyte fractions (D). *p < 0.001.

(E and F) In vitro pericyte lineage tracing of GSCs with Desmin promoter-driven GFP induced by serum or TGF-β (2 ng/ml). Quantification shows fractions of GFP+ cells in the differentiated cells (F). *p < 0.001

(G) In vitro HBMEC complex formation with DesPro-GFP-GSCs in the presence of anti-TGFβ antibody (monoclonal antibody [mAb]) or immunoglobulin G (IgG).

(H) IB analysis of α -SMA expression after coculture of GSCs with HBMECs or their conditioned media in the presence of anti-TGF- β antibody or IgG.

(I) A schematic illustration showing the recruitment of GSCs toward ECs and the differentiation of GSCs into pericytes in GBMs. GSCs expressing CXCR4 are recruited toward ECs by SDF-1 and induced predominantly by TGF-\$\beta\$ to become pericytes to support vessel function and tumor growth. The scale bars represent 25 μm (C and E) and 100 μm (G). The error bars represent SD.

directly demonstrated that GSCs give rise to pericytes rather than ECs in vivo.

The contribution of GSCs to vascular pericytes requires GSC recruitment toward ECs. Because ECs in brain and GBMs express abundant SDF-1 forming chemoattractant gradient, the expression of CXCR4 (the receptor for SDF-1) in

GSCs (Ehtesham et al., 2009; Folkins et al., 2009) may provide a paracrine loop for recruitment of GSCs toward ECs. A recent study showed that NSCs can be recruited to perivascular niches in normal brain through the CXCR4/SDF-1 axis (Kokovay et al., 2010). The recruitment of pericyte progenitors to ECs in normal tissues also depends on SDF-1/CXCR4 signaling (Song et al., 2009). SDF-1 expression has been proposed as one of the mechanisms underlying the resistance to antiangiogenic therapy in GBM trials (Batchelor et al., 2007). Elevated SDF-1 signaling may enhance GSC recruitment toward ECs and increase G-pericyte coverage to protect tumor vessels, leading to resistance to antiangiogenic therapy.

The potent capacity of GSCs to generate vascular pericytes allows active vascularization in GBMs to support tumor growth. Because GSCs contribute to the majority of vascular pericytes in GBMs, G-pericytes may have a crucial role in mediating therapeutic resistance in GBMs. Because pericytes juxtacrine to ECs express significant levels of VEGF and other factors to support EC survival (Franco et al., 2011; Song et al., 2005; Winkler et al., 2011), G-pericytes may protect ECs and render ECs less responsive to antiangiogenic agents in GBMs. Thus, targeting G-pericytes may synergize with current therapies targeting ECs to achieve more effective outcome. Because CSCs are present in other solid cancers (Magee et al., 2012), it is important to determine whether CSCs can generate vascular pericytes in other malignant tumors with florid angiogenesis. Our studies demonstrate that GSCs not only interact with perivascular niches but also have the capacity to remodulate their microenvironment by contributing pericyte compartments of the neovasculature. Because selective elimination of G-pericytes potently disrupted vessels and inhibited tumor growth, therapeutic targeting of G-pericytes may have a significant impact on improving GBM treatment efficacy.

EXPERIMENTAL PROCEDURES

Isolation of GSCs and Non-Stem Tumor Cells from GBMs

GBM surgical specimens were collected in accordance with a Cleveland Clinic Institutional Review Board-approved protocol. GSCs and non-stem tumor cells were derived from GBM tumors and functionally validated as described previously (Bao et al., 2006a; Guryanova et al., 2011). For the detailed procedure, please see Extended Experimental Procedures.

Pericyte or EC-Specific Promoter-Driven Expression of GFP or **mCherry**

Human Desmin promoter (312 bp) with an enhancer (284 bp) (Li and Paulin, 1991), α-SMA promoter (262 bp) with an enhancer (123 bp) (Keogh et al., 1999; Nakano et al., 1991), CD105 promoter plus enhancer (955 bp) (Ríus et al., 1998), and CD31 promoter plus enhancer (887 bp) restricted to ECs (Almendro et al., 1996; Gumina et al., 1997) were cloned by PCR and confirmed by sequencing. The specific promoter with enhancer was inserted into pCDH-CMV-EF1-Puro lentiviral vector (System Biosciences) to replace the original CMV promoter. The ORF of GFP or mCherry was then inserted into the vector to generate lentiviral constructs. Lentiviruses were produced and tittered as described elsewhere (Guryanova et al., 2011).

Cell Lineage Tracing of GSCs

To perform cell lineage tracing, GSCs were transduced with GFP or mCherry constitutive expression or conditional expression driven by the pericyte or EC-specific promoter through lentiviral infection and then transplanted into brains of athymic BALB/c nu/nu mice to establish xenografts as described elsewhere (Guryanova et al., 2011). To trace cell lineage of GSCs in vivo, sections of mouse brains bearing the xenografts were immunostained for pericyte or EC markers and analyzed for GFP or mCherry expression. IF and IHC stainings were performed as described (Guryanova et al., 2011). Tumor sections of the genetically engineered mouse GBMs were provided by Dr. Dolores Hambardzumyan. For detailed methods and the antibody information, please see Extended Experimental Procedures.

Selective Targeting of G-Pericytes in GBM Xenografts

GSCs were transduced with Desmin or CD31-promoter-driven expression of HsvTK, GFP, or HsvTK plus GFP through lentiviral infection and then transplanted into brains of athymic mice. Mice bearing the xenografts received GCV (Sigma-Aldrich) at 75 mg/kg/day or vehicle control daily through intraperitoneal injection. The xenografts were collected for IF and IHC staining and fluorescent analysis. To evaluate the targeting effect on animal survival, mice were maintained until the development of neurological signs.

HBVPs, HBMECs, and EC Complex Formation

HBVPs and HBMECs were obtained from ScienCell. HBMECs with low passage were used for coculture and endothelial complex formation assays as described (Bao et al., 2006b). For the detailed procedure and the labeling of GSCs and HBMECs, please see Extended Experimental Procedures.

Statistical Analysis

All quantified data were statistically analyzed. Grouped data are presented as mean \pm SD. The difference between experimental groups was assessed by one-way ANOVA or one-way ANOVA on ranks testing. For the animal survival experiments, log-rank survival analysis was performed.

For further details, please see Extended Experimental Procedures.

SUPPLEMENTAL INFORMATION

Supplemental Information includes Extended Experimental Procedures, seven figures, and one table and can be found with this article online at http://dx.doi. org/10.1016/j.cell.2013.02.021.

ACKNOWLEDGMENTS

We thank Brain Tumor and Neuro-Oncology Centers at Cleveland Clinic, University Hospitals, and Duke Medical Center for providing GBM specimens. We also thank Dr. Dolores Hambardzumyan for providing the genetically engineered mouse GBMs. We are grateful to Cathy Shemo at the Flow Cytometry Core and Judith Drazba at the Imaging Core for their help. This work was supported by the Cleveland Clinic Foundation and National Institutes of Health R01 grant NS070315 (to S.B.).

Received: August 19, 2011 Revised: May 12, 2012 Accepted: February 11, 2013 Published: March 28, 2013

REFERENCES

Almendro, N., Bellón, T., Rius, C., Lastres, P., Langa, C., Corbí, A., and Bernabéu, C. (1996). Cloning of the human platelet endothelial cell adhesion molecule-1 promoter and its tissue-specific expression. Structural and functional characterization. J. Immunol. 157, 5411-5421.

Armulik, A., Genové, G., Mäe, M., Nisancioglu, M.H., Wallgard, E., Niaudet, C., He, L., Norlin, J., Lindblom, P., Strittmatter, K., et al. (2010). Pericytes regulate the blood-brain barrier. Nature 468, 557-561.

Bao, S., Wu, Q., McLendon, R.E., Hao, Y., Shi, Q., Hjelmeland, A.B., Dewhirst, M.W., Bigner, D.D., and Rich, J.N. (2006a). Glioma stem cells promote radioresistance by preferential activation of the DNA damage response. Nature 444, 756-760.

Bao, S., Wu, Q., Sathornsumetee, S., Hao, Y., Li, Z., Hjelmeland, A.B., Shi, Q., McLendon, R.E., Bigner, D.D., and Rich, J.N. (2006b). Stem cell-like glioma cells promote tumor angiogenesis through vascular endothelial growth factor. Cancer Res. 66, 7843-7848.

Batchelor, T.T., Sorensen, A.G., di Tomaso, E., Zhang, W.T., Duda, D.G., Cohen, K.S., Kozak, K.R., Cahill, D.P., Chen, P.J., Zhu, M., et al. (2007). AZD2171, a pan-VEGF receptor tyrosine kinase inhibitor, normalizes tumor vasculature and alleviates edema in glioblastoma patients. Cancer Cell 11,

Bell, R.D., Winkler, E.A., Sagare, A.P., Singh, I., LaRue, B., Deane, R., and Zlokovic, B.V. (2010). Pericytes control key neurovascular functions and neuronal phenotype in the adult brain and during brain aging. Neuron 68, 409-427.

Bergers, G., and Song, S. (2005). The role of pericytes in blood-vessel formation and maintenance. Neuro-oncol. 7, 452-464.

Bergers, G., Song, S., Meyer-Morse, N., Bergsland, E., and Hanahan, D. (2003). Benefits of targeting both pericytes and endothelial cells in the tumor vasculature with kinase inhibitors. J. Clin. Invest. 111, 1287-1295.

Calabrese, C., Poppleton, H., Kocak, M., Hogg, T.L., Fuller, C., Hamner, B., Oh, E.Y., Gaber, M.W., Finklestein, D., Allen, M., et al. (2007). A perivascular niche for brain tumor stem cells. Cancer Cell 11, 69-82.

Cancer Genome Atlas Research Network. (2008). Comprehensive genomic characterization defines human glioblastoma genes and core pathways. Nature 455, 1061-1068,

Carmeliet, P., and Jain, R.K. (2011). Principles and mechanisms of vessel normalization for cancer and other angiogenic diseases. Nat. Rev. Drug Discov. 10, 417-427.

Crisan, M., Yap, S., Casteilla, L., Chen, C.W., Corselli, M., Park, T.S., Andriolo, G., Sun, B., Zheng, B., Zhang, L., et al. (2008). A perivascular origin for mesenchymal stem cells in multiple human organs. Cell Stem Cell 3, 301-313.

Culver, K.W., Ram, Z., Wallbridge, S., Ishii, H., Oldfield, E.H., and Blaese, R.M. (1992). In vivo gene transfer with retroviral vector-producer cells for treatment of experimental brain tumors. Science 256, 1550-1552.

deCarvalho, A.C., Nelson, K., Lemke, N., Lehman, N.L., Arbab, A.S., Kalkanis, S., and Mikkelsen, T. (2010). Gliosarcoma stem cells undergo glial and mesenchymal differentiation in vivo. Stem Cells 28, 181-190.

De Palma, M., Venneri, M.A., Galli, R., Sergi Sergi, L., Politi, L.S., Sampaolesi, M., and Naldini, L. (2005). Tie2 identifies a hematopoietic lineage of proangiogenic monocytes required for tumor vessel formation and a mesenchymal population of pericyte progenitors. Cancer Cell 8, 211-226.

Du, R., Lu, K.V., Petritsch, C., Liu, P., Ganss, R., Passegué, E., Song, H., Vandenberg, S., Johnson, R.S., Werb, Z., and Bergers, G. (2008). HIF1alpha induces the recruitment of bone marrow-derived vascular modulatory cells to regulate tumor angiogenesis and invasion. Cancer Cell 13, 206-220.

Ehtesham, M., Mapara, K.Y., Stevenson, C.B., and Thompson, R.C. (2009). CXCR4 mediates the proliferation of glioblastoma progenitor cells. Cancer Lett. 274, 305-312.

Folkins, C., Shaked, Y., Man, S., Tang, T., Lee, C.R., Zhu, Z., Hoffman, R.M., and Kerbel, R.S. (2009). Glioma tumor stem-like cells promote tumor angiogenesis and vasculogenesis via vascular endothelial growth factor and stromal-derived factor 1. Cancer Res. 69, 7243-7251.

Franco, M., Roswall, P., Cortez, E., Hanahan, D., and Pietras, K. (2011). Pericytes promote endothelial cell survival through induction of autocrine VEGF-A signaling and Bcl-w expression. Blood 118, 2906–2917.

Gerhardt, H., Wolburg, H., and Redies, C. (2000). N-cadherin mediates pericytic-endothelial interaction during brain angiogenesis in the chicken. Dev. Dyn. 218, 472-479.

Gumina, R.J., Kirschbaum, N.E., Piotrowski, K., and Newman, P.J. (1997). Characterization of the human platelet/endothelial cell adhesion molecule-1 promoter: identification of a GATA-2 binding element required for optimal transcriptional activity. Blood 89, 1260-1269.

Guryanova, O.A., Wu, Q., Cheng, L., Lathia, J.D., Huang, Z., Yang, J., MacSwords, J., Eyler, C.E., McLendon, R.E., Heddleston, J.M., et al. (2011). Nonreceptor tyrosine kinase BMX maintains self-renewal and tumorigenic potential of glioblastoma stem cells by activating STAT3. Cancer Cell 19, 498-511.

Hambardzumyan, D., Amankulor, N.M., Helmy, K.Y., Becher, O.J., and Holland, E.C. (2009). Modeling adult gliomas using RCAS/t-va technology. Transl. Oncol. 2, 89-95.

li, M., Nishimura, H., Sekiguchi, H., Kamei, N., Yokoyama, A., Horii, M., and Asahara, T. (2009). Concurrent vasculogenesis and neurogenesis from adult neural stem cells. Circ. Res. 105, 860-868.

Keogh, M.C., Chen, D., Schmitt, J.F., Dennehy, U., Kakkar, V.V., and Lemoine, N.R. (1999). Design of a muscle cell-specific expression vector utilising human vascular smooth muscle alpha-actin regulatory elements. Gene Ther. 6, 616-628.

Kokovay, E., Goderie, S., Wang, Y., Lotz, S., Lin, G., Sun, Y., Roysam, B., Shen, Q., and Temple, S. (2010). Adult SVZ lineage cells home to and leave the vascular niche via differential responses to SDF1/CXCR4 signaling. Cell Stem Cell 7, 163-173.

Komatani, H., Sugita, Y., Arakawa, F., Ohshima, K., and Shigemori, M. (2009). Expression of CXCL12 on pseudopalisading cells and proliferating microvessels in glioblastomas: an accelerated growth factor in glioblastomas. Int. J. Oncol. 34, 665-672.

Kulla, A., Burkhardt, K., Meyer-Puttlitz, B., Teesalu, T., Asser, T., Wiestler, O.D., and Becker, A.J. (2003). Analysis of the TP53 gene in laser-microdissected glioblastoma vasculature. Acta Neuropathol. 105, 328-332.

Li, Z.L., and Paulin, D. (1991). High level desmin expression depends on a muscle-specific enhancer. J. Biol. Chem. 266, 6562-6570.

Magee, J.A., Piskounova, E., and Morrison, S.J. (2012). Cancer stem cells: impact, heterogeneity, and uncertainty. Cancer Cell 21, 283-296.

Morikawa, S., Baluk, P., Kaidoh, T., Haskell, A., Jain, R.K., and McDonald, D.M. (2002). Abnormalities in pericytes on blood vessels and endothelial sprouts in tumors. Am. J. Pathol. 160, 985-1000.

Morishita, R., Nagata, K., Ito, H., Ueda, H., Asano, M., Shinohara, H., Kato, K., and Asano, T. (2007). Expression of smooth muscle cell-specific proteins in neural progenitor cells induced by agonists of G protein-coupled receptors and transforming growth factor-beta. J. Neurochem. 101, 1031-1040.

Nakano, Y., Nishihara, T., Sasayama, S., Miwa, T., Kamada, S., and Kakunaga, T. (1991). Transcriptional regulatory elements in the 5' upstream and first intron regions of the human smooth muscle (aortic type) alpha-actin-encoding gene. Gene 99, 285-289.

Norden, A.D., Drappatz, J., and Wen, P.Y. (2009). Antiangiogenic therapies for high-grade glioma. Nat. Rev. Neurol. 5, 610-620.

Pàez-Ribes, M., Allen, E., Hudock, J., Takeda, T., Okuyama, H., Viñals, F., Inoue, M., Bergers, G., Hanahan, D., and Casanovas, O. (2009). Antiangiogenic therapy elicits malignant progression of tumors to increased local invasion and distant metastasis. Cancer Cell 15, 220-231.

Ricci-Vitiani, L., Pallini, R., Larocca, L.M., Lombardi, D.G., Signore, M., Pierconti, F., Petrucci, G., Montano, N., Maira, G., and De Maria, R. (2008). Mesenchymal differentiation of glioblastoma stem cells. Cell Death Differ. 15. 1491-1498.

Ricci-Vitiani, L., Pallini, R., Biffoni, M., Todaro, M., Invernici, G., Cenci, T., Maira, G., Parati, E.A., Stassi, G., Larocca, L.M., and De Maria, R. (2010). Tumour vascularization via endothelial differentiation of glioblastoma stemlike cells. Nature 468, 824-828.

Ríus, C., Smith, J.D., Almendro, N., Langa, C., Botella, L.M., Marchuk, D.A., Vary, C.P., and Bernabéu, C. (1998). Cloning of the promoter region of human endoglin, the target gene for hereditary hemorrhagic telangiectasia type 1. Blood 92, 4677-4690.

Rodriguez, F.J., Orr, B.A., Ligon, K.L., and Eberhart, C.G. (2012). Neoplastic cells are a rare component in human glioblastoma microvasculature. Oncotar-

Soda, Y., Marumoto, T., Friedmann-Morvinski, D., Soda, M., Liu, F., Michiue, H., Pastorino, S., Yang, M., Hoffman, R.M., Kesari, S., and Verma, I.M. (2011). Transdifferentiation of glioblastoma cells into vascular endothelial cells. Proc. Natl. Acad. Sci. USA 108, 4274-4280.

Song, S., Ewald, A.J., Stallcup, W., Werb, Z., and Bergers, G. (2005). PDGFRbeta+ perivascular progenitor cells in tumours regulate pericyte differentiation and vascular survival. Nat. Cell Biol. 7, 870-879.

Song, N., Huang, Y., Shi, H., Yuan, S., Ding, Y., Song, X., Fu, Y., and Luo, Y. (2009). Overexpression of platelet-derived growth factor-BB increases tumor pericyte content via stromal-derived factor-1alpha/CXCR4 axis. Cancer Res. 69.6057-6064.

Verhaak, R.G., Hoadley, K.A., Purdom, E., Wang, V., Qi, Y., Wilkerson, M.D., Miller, C.R., Ding, L., Golub, T., Mesirov, J.P., et al.; Cancer Genome Atlas Research Network. (2010). Integrated genomic analysis identifies clinically relevant subtypes of glioblastoma characterized by abnormalities in PDGFRA, IDH1. EGFR. and NF1. Cancer Cell 17. 98-110.

Wang, R., Chadalavada, K., Wilshire, J., Kowalik, U., Hovinga, K.E., Geber, A., Fligelman, B., Leversha, M., Brennan, C., and Tabar, V. (2010). Glioblastoma stem-like cells give rise to tumour endothelium. Nature 468, 829-833.

Winkler, E.A., Bell, R.D., and Zlokovic, B.V. (2011). Central nervous system pericytes in health and disease. Nat. Neurosci. 14, 1398-1405.

Zhou, B.B., Zhang, H., Damelin, M., Geles, K.G., Grindley, J.C., and Dirks, P.B. (2009). Tumour-initiating cells: challenges and opportunities for anticancer drug discovery. Nat. Rev. Drug Discov. 8, 806-823.

Supplemental Information

EXTENDED EXPERIMENTAL PROCEDURES

Isolation of GSCs and Non-Stem Tumor Cells from GBMs

GBM surgical specimens were collected for this study in accordance with a Cleveland Clinic Institutional Review Board-approved protocol. GSCs and non-stem tumor cells (non-stem TCs) were derived from GBM surgical specimens or xenografts and characterized as previously described (Bao et al., 2006a, 2008; Guryanova et al., 2011; Li et al., 2009) with minor modification. Briefly, GBM tumors were disaggregated using the Papain Dissociation System (Worthington Biochemical) according to the manufacturer's instructions. Isolated cells were recovered in stem cell medium (Neurobasal-A medium with B27 supplement, 10 ng/ml EGF and 10 ng/ml bFGF) for at least 6 hr to allow re-expression of surface markers, and then sorted by fluorescence-activated cell sorting (FACS) or magnetic cell sorting for GSCs using at least two surface markers (CD15/CD133, or CD15/L1CAM). The enriched GSCs were maintained in the stem cell medium and confirmed by SOX2 and OLIG2 expression and GSC ability to turn on the SOX2 promoter-driven GFP expression. The cancer stem cell phenotype of GSCs was validated by functional assays of self-renewal (serial neurosphere passage), in vitro differentiation and tumor propagation (in vivo limiting dilution assay) as previously described (Guryanova et al., 2011; Li et al., 2009). To avoid any pericyte contamination in GSCs, the sorted GSCs from primary GBMs were subjected to secondary sorting (negative selection for CD146 and CD248) using FITC-conjugated anti-CD248 and PE-conjugated anti-CD146 (BD Bioscience), and the isolated GSCs from GBM xenografts were subjected to the secondary selection positive for TRA-1-85 (a human cell-specific surface antigen) and negative for CD146 using FITC-conjugated anti-TRA-1-85 and PE-conjugated anti-CD146. To generate single GSC-derived tumorspheres, the sorted GSCs were seeded in 96-well plates by serial dilution or by the FACS sorter. The single GSC-generated neurosphere from each well was transferred into new well in a 24 well plate for the in vitro differentiation assay. The freshly sorted GSCs from GBM surgical specimens or xenografts and the derived GSC tumorspheres were used for in vitro or in vivo experiments as indicated.

Cardiac Perfusion for Collection of Mouse Brains

Prior to the collection of mouse brains bearing the tumors, cardiac perfusion with PBS followed by perfusion with 4% PFA (Paraformaldehyde, Sigma-Aldrich) was performed. Tumors were fixed with 4% PFA overnight at 4°C, post-fixed in 70% ethanol, cryopreserved in 30% sucrose and cryosectioned for staining and fluorescent analysis, or embedded with paraffin and cut for histological and IHC staining.

Immunofluorescence, Immunohistochemistry, and Immunoblot Analysis

IF staining was performed as previously described (Guryanova et al., 2011; Huang et al., 2011). Briefly, cultured cells or frozen sections of tumorspheres, GBM xenografts, surgical specimens or the genetically engineered mouse GBMs were fixed with 4% paraformaldehyde (PFA, Sigma-Aldrich) for 15 min then blocked with 10% normal goat serum (Vector) with or without 0.1% Triton X-100 (Bio-Rad) in PBS for 30 min at room temperature. Samples were incubated with primary antibodies overnight at +4°C followed by the appropriate secondary fluorescently labeled antibodies (Invitrogen Molecular Probes) for one hour at room temperature. Nuclei were counterstained with DAPI. Images were taken with a wide-field fluorescence microscope (Leica) or Leica SP-5 confocal microscope. Immunohistochemical (IHC) staining to examine blood vessel density in GBM xenografts was performed with an ABC kit using DAB detection as described previously (Bao et al., 2006b; Guryanova et al., 2011). Immunoblot analysis was performed as previously described (Guryanova et al., 2011; Huang et al., 2011). Cells were lysed in RIPA buffer supplemented with protease and phosphatase inhibitors (Roche). Precleared protein samples were resolved by SDS-PAGE and blotted onto nitrocellulose membranes. After blocking in milk-based buffer, blots were incubated with primary antibodies overnight at 4°C followed by HRP-linked species-specific antibodies (Santa-Cruz). Specific antibodies against CD31/PECAM-1 (Bethyl laboratories or Dako), Glut1 (Millipore), Desmin (Dako or Santa Cruz), α-SMA (Dako), NG2 (CSPG4) (Millipore), PDGFRβ (Cell Signaling), CD248 (TEM1) (Millipore or Santa Cruz), CD146 (BD Bioscience), Connexin45 (Millipore), Ang1 (Abcam), CD13 (BD Bioscience), GFAP (Covance), S100β (BD Bioscience), SOX2 (Millipore or Santa Cruz), Nestin (BD Bioscience), OLIG2 (R&D System), HA (Roche) and NuMA (Santa Cruz) were used for the IF staining, IHC or immunoblot analysis.

Analysis of Vessel Density, Pericyte Coverage, and Vessel Function

Vessel density and pericyte coverage were analyzed as described (Bao et al., 2006b; Nolan-Stevaux et al., 2010). Vascular or pericyte area was measured and percentage of pixel overlap was analyzed. To test vessel function, mice bearing GBM xenografts were perfused with FITC-conjugated mega-dextran (MW = 2,000 KDa, Invitrogen) for 30-60 min, and then harvested for fluorescent analysis and quantification of the perfused FITC-mega-dextran (in green) as described (Bell et al., 2010).

shRNA Lentiviruses and Lentiviral Infection

CXCR4 shRNA clones in lentiviral vector (Mission shRNA, Sigma-Aldrich) were used to reduce CXCR4 expression in GSCs through lentiviral infection. Lentiviruses expressing CXCR4 shRNA (shCXCR4) or nontargeting shRNA (shNT) were produced in 293FT cells with pPACK set of helper plasmids (System Biosciences) and then titered as described previously (Guryanova et al., 2011; Li et al., 2009). The viruses were concentrated by precipitation with polyethylene glycol 8000 (PEG8000) (Fisher Scientific). GSCs transduced with shCXCR4 or shNT were used for the in vitro EC complex formation or the in vivo pericyte lineage tracing experiments.

Endothelial Complex Formation and Coculture of ECs with GSCs

To examine the role of G-pericytes in supporting endothelial complexes, HBMECs were prelabeled with red fluorescent cell tracer CMTPX (Invitrogen) and then allowed to form EC complexes. CFSE-labeled GSCs (green) or GFP-expressing GSCs were then added to the established EC complexes, and then monitored and photographed under the EVOS fluorescent microscope over time (day 0 to day 8). The expression of α -SMA (a pericyte marker) and N-cadherin in the EC complex with GSC-derived cells was detected by immunofluorescent staining with anti- α -SMA (Dako) and anti-N-cadherin (Santa Cruz) antibodies. To investigate the impact of CXCR4 knockdown on GSC recruitment to EC complexes, GFP-labeled GSCs expressing CXCR4-targeting shRNA (shCXCR4) or nontargeting shRNA (shNT) were added to the established EC complexes, and the integration of GSC-derived cells (GFP+) into EC complexes was monitored, photographed and then quantified. To examine the effect of CXCR4 inhibitor AMD3100 on recruitment of GSCs to EC complexes, HBMECs were prelabeled with the green fluorescent cell tracer CFSE (Invitrogen) and allowed to form complexes, and GSCs labeled with the red fluorescent cell tracer CMTPX (Invitrogen) were added to the HBMEC complexes without or with AMD3100 at 1 μ g/ml concentration. The recruitment and integration of GSCs (in red) to the EC complexes (in green) was monitored and analyzed.

In Vitro Matrigel Cell Migration Assay

The cell migration of GSCs toward cytokines or ECs through the Matrigel (BD Bioscience) in vitro was performed as described previously (Bao et al., 2006b). GSCs were added on upper chambers of the transwells, and cytokines (SDF-1, TGF- β or PDGFB) or HBMECs with/without anti-TGF β mAb was put in the bottom chambers in the assay. Cells migrated through the BD Matrigel were stained and counted.

Fluorescence Immunophenotyping and Interphase Cytogenetics

Fluorescence in situ hybridization (FISH) analysis in combination with IF staining (Fluorescence Immunophenotyping and Interphase Cytogenetics) was performed as described (Calabrese et al., 2007; Ricci-Vitiani et al., 2008). Sections of GBM specimens or tissue arrays (Duke Brain Tumor Center and US Biomax) were immunostained for α -SMA to mark pericytes or CD31 to label ECs, and then followed by FISH detection. Locus-specific probes (FITC-labeled or PE-conjugated CEP-7, CEP-10, EGFR or PTEN; Vysis) were used according to the manufacturer's instructions.

Detection of Apoptosis in G-Pericytes Expressing HsvTK

In vitro apoptosis was detected with the PE-Annexin V staining kit (BD Bioscience). The detection of the GCV-induced apoptosis in G-pericytes expressing HsvTK in GBM xenografts by TUNEL assay was carried out with an in situ cell apoptosis kit (Cell Signaling).

Isolation of Pericytes and ECs from GBM Tumors

Pericytes and ECs were isolated from GBM tumors using fluorescence-activated cell sorting (FACS) (Crisan et al., 2008; Milner et al., 2008). The pericytes were sorted from total cells of primary GBMs by selecting CD146+CD248+CD34- cells through positive sorting with PE-conjugated anti-CD146 and FITC-conjugated anti-CD248 antibodies, and then negative sorting with PE-conjugated anti-CD34 antibody (BD Bioscience). The G-pericytes from the DesPro-GFP-GSC xenografts were sorted by selecting GFP+CD146+ cells using PE-conjugated anti-CD146 antibody and GFP fluorescence. ECs from GBM tumors were sorted by selecting CD31+CD105+ cells with FITC-conjugated anti-CD105 and PE-conjugated anti-CD31 antibodies (BD Bioscience).

Induction of GSC Differentiation In Vitro

The freshly isolated GSCs or the single GSC-derived tumorspheres were induced for differentiation in DMEM with FBS (1%–10%) as indicated. In some experiments, cytokine TGF- β 1 (R&D systems), PDGF-B (Cell Signaling) or SDF-1 (R&D systems) were added to the culture. The differentiated cells were harvested for IF staining or immunoblot analysis to examine the expression of cell lineage markers.

RT-PCR Analysis of Pericyte and GSC Markers

To confirm the expression of pericyte markers in G-pericytes and examine whether G-pericytes express GSC or NSC markers, RNA samples were isolated from the sorted G-pericytes (GFP+CD146+) from DesPro-GFP GSC xenografts, normal human brain vascular pericytes (HBVPs) and GSCs using a RNA isolation kit (QIAGEN), and then subjected to RT-PCR analyses with pairs of primers for pericyte markers and GSC or NSC markers. Primers for pericyte markers: α-SMA (forward: 5′ TAG CAC CCA GCA CCA TGA AGA TCA 3′, reverse: 5′ GAA GCA TTT GCG GTG GAC AAT GGA 3′); Desmin (forward: 5′ AAA TCC GGC ACC TCA AGG ATG AGA 3′, reverse: 5′ TTT CTC GGA AGT TGA GGG CAG AGT 3′); CD146 (forward: 5′ TGG CAT TCA AGG AGA GGA AGG TGT 3′, reverse: 5′ ACT CGC TGT GGA TCT TGG TCT TGT 3′); NG2 (CSPG4) (forward: 5′ AGC TCT ACT CTG GAC GCC 3′, reverse: 5′ ATC GAC TGA CAA CGT GGC 3′); CD248 (forward: 5′ AGA CCA CCA CTCA TTT GCC TGG AA 3′, reverse: 5′ AGT TGG GAT AAT GGG AAG CTG GGT 3′); PGDFRβ (forward: 5′ ACG GCT CTA CAT CTT TGT GCC AGA 3′, reverse: 5′ TCG GCA TGG AAT GGT GAT CTC AGT 3′). Primers for GSC or NSC markers: OLIG2 (forward: 5′ CAA GAA GCA AAT GAC AGA GCC GGA 3′, reverse: 5′ TGG GCA TGG ATC TCC GAG TTG TGG 3′); CD133 (forward: 5′ CTT ACG GCA CTC TTC ACC TG 3′, reverse: 5′ TCC CTG TGC GTT GAA GTA TC 3′); Nestin

(forward: 5' TGC GGG CTA CTG AAA AGT TC 3', reverse: 5' TGA AAG CTG AGG GAA GTC TTG 3'). Primers for control proteins: GFP (forward: 5' AGA TTC GAG AAA CCA GCC TGG ACA 3', reverse: 5' TTG TGC TCC TGC TTG GAC TCC TTA 3'); and GAPDH (forward: 5' TGT TGC CAT CAA TGA CCC CTT 3', reverse: 5' CTC CAC GAC GTA CTC AGC G 3').

SUPPLEMENTAL REFERENCES

Bao, S., Wu, Q., Li, Z., Sathornsumetee, S., Wang, H., McLendon, R.E., Hjelmeland, A.B., and Rich, J.N. (2008). Targeting cancer stem cells through L1CAM suppresses glioma growth. Cancer Res. 68, 6043-6048.

Huang, Z., Wu, Q., Guryanova, O.A., Cheng, L., Shou, W., Rich, J.N., and Bao, S. (2011). Deubiquitylase HAUSP stabilizes REST and promotes maintenance of neural progenitor cells. Nat. Cell Biol. 13, 142-152.

Li, Z., Bao, S., Wu, Q., Wang, H., Eyler, C., Sathornsumetee, S., Shi, Q., Cao, Y., Lathia, J., McLendon, R.E., et al. (2009). Hypoxia-inducible factors regulate tumorigenic capacity of glioma stem cells. Cancer Cell 15, 501–513.

Milner, R., Hung, S., Wang, X., Spatz, M., and del Zoppo, G.J. (2008). The rapid decrease in astrocyte-associated dystroglycan expression by focal cerebral ischemia is protease-dependent. J. Cereb. Blood Flow Metab. 28, 812-823.

Nolan-Stevaux, O., Truitt, M.C., Pahler, J.C., Olson, P., Guinto, C., Lee, D.C., and Hanahan, D. (2010). Differential contribution to neuroendocrine tumorigenesis of parallel egfr signaling in cancer cells and pericytes. Genes Cancer 1, 125–141.

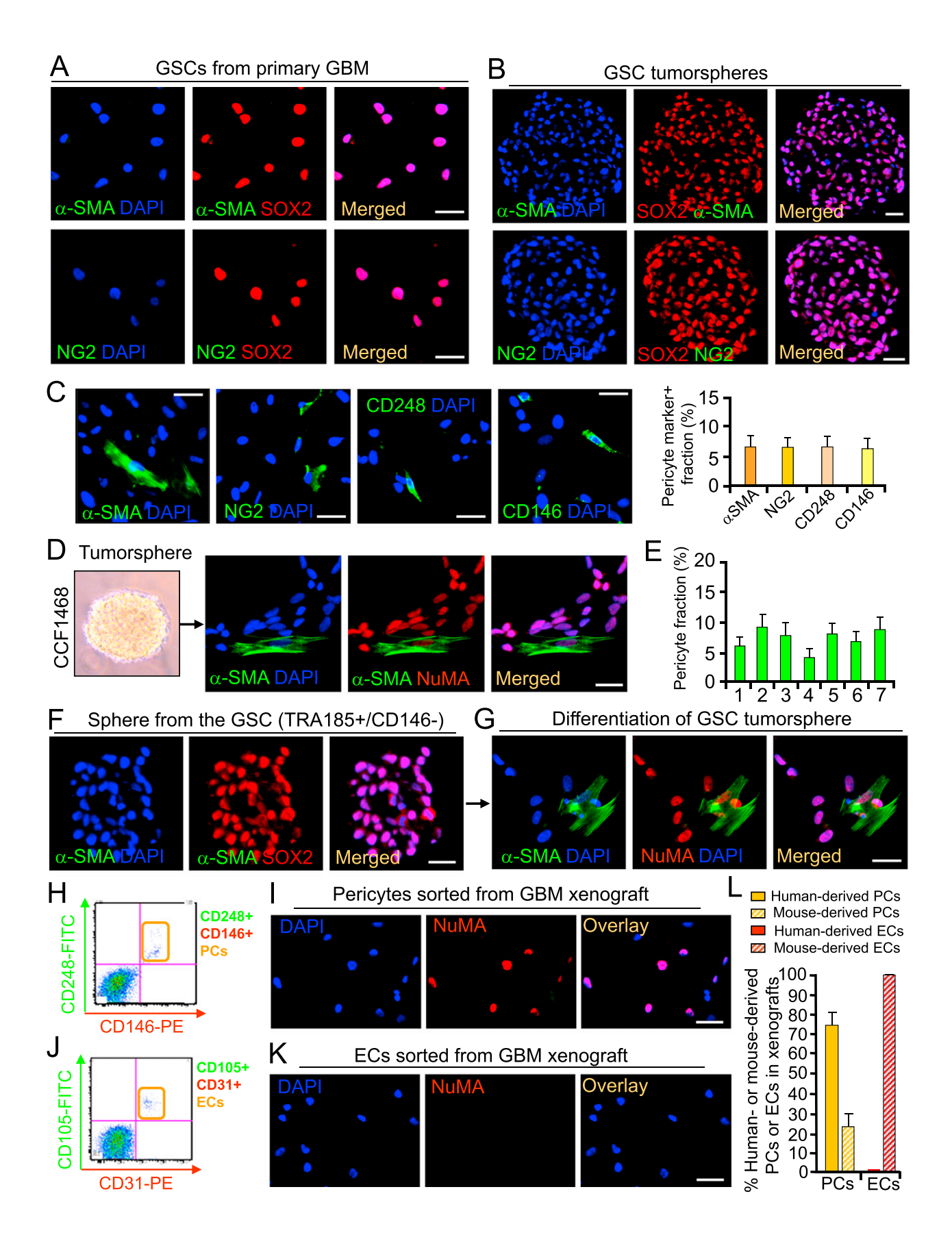


Figure S1. GBM Stem Cells Are Able to Differentiate into Pericytes In Vitro, Related to Figure 1

(A) IF staining of the GSC marker (SOX2) and pericyte marker (α-SMA or NG2) in the freshly isolated GSCs from a primary GBM (CW1326). The sorted GSCs were immunostained with specific antibodies against the GSC marker SOX2 (in red) and a pericyte marker (α-SMA or NG2, in green), and then counterstained with DAPI. The sorted GSCs express SOX2 but do not contain any cell positive for the pericyte markers.

(B) IF staining of pericyte marker (α-SMA or NG2) and the GSC marker (SOX2) in GSC tumorspheres. Frozen sections of GSC tumorspheres derived from GSCs from a primary GBM (CW1217) were immunostained with specific antibodies against a pericyte marker (α-SMA or NG2, in green) and a GSC marker (SOX2, in red), and then counterstained with DAPI to mark nuclei (in blue). The majority (91%-96%) of cells in GSC tumorspheres expressed SOX2 but no cell in the tumorspheres expressed the pericyte markers.

(C) IF staining of pericyte markers (α-SMA, NG2, CD146 and CD248) in the differentiated cells derived from the freshly isolated GSCs from a human primary GBM (CCF2049). The sorted GSCs were cultured in DMEM with 10% FBS for 6 days, then immunostained with specific antibodies against the indicated pericyte markers (in green) and counterstained with DAPI to mark nuclei (in blue). Quantification on right side shows fractions of the differentiated cells expressing the pericyte markers. The differentiation experiments were done four times and 300 cells were counted each time for each pericyte marker.

(D and E) IF staining of α-SMA and NuMA (a human cell-specific nuclear antigen) in the differentiated cells derived from GSC tumorspheres. The cells from single tumorsphere derived from GSC (CCF1468) were induced for differentiation in DMEM with 10% FBS for 6 days. The differentiated cells were immunostained with specific antibodies against α-SMA (in green) and the human cell-specific nuclear antigen NuMA (in red) to mark human cells, and counterstained with DAPI (in blue). Quantification (E) shows that the differentiated cells contain a fraction (4%-11%) of cells expressing the pericyte marker.

(F) IF staining of α-SMA (in green) and SOX2 (in red) in the single GSC-generated tumorspheres derived from the GSCs without host-derived pericyte. The freshly sorted GSCs from a GBM xenograft (T3691) were subjected for secondary selection positive for TRA-1-85 (a human cell-specific surface antigen) and negative for CD146 by using the FITC-conjugated anti-TRA-1-85 and the PE-conjugated anti-CD146. Frozen sections of the single GSC-derived tumorspheres from the GSCs (TRA185⁺CD146-) after the double sorting were immunostained with specific antibodies against the pericyte marker (α-SMA, in green) and a GSC marker (SOX2, in red), and then counterstained with DAPI (in blue). All cells in the tumorspheres are negative for the pericyte marker α-SMA but most cells show SOX2

(G) IF staining of α-SMA (in green) and NuMA (a human cell-specific nuclear antigen, in red) in the differentiated cells from the single GSC-generated tumorsphere described in (F). Cells were counterstained with DAPI (in blue). The differentiated cells are all NuMA positive and contain a fraction (4%-11%) of cells expressing the pericyte marker α -SMA.

- (H) FACS sorting of pericyte population (CD146+CD248+) from a GBM xenograft. The pericytes were isolated from total cells derived from GBM xenografts (T3359) through cell sorting with the PE-conjugated anti-CD146 and the FITC-conjugated anti-248 specific antibodies.
- (I) IF staining of NuMA (in red) in the freshly sorted pericyte population (CD146*CD248*) described in (H). Cells were counterstained with DAPI to show nuclei (in blue). The human cell-specific nuclear antigen NuMA (in red) was expressed in the majority of sorted pericytes from the GBM xenografts.
- (J) FACS sorting of endothelial cell (EC) population (CD31*CD105*) from a GBM xenograft. The ECs were isolated from total cells derived from GBM xenografts (T3359) through cell sorting with PE-conjugated anti-CD31 and the FITC-conjugated anti-105 antibodies.
- (K) IF staining of NuMA (in red) in the freshly sorted EC population (CD31*CD105*) described in (J). Cells were counterstained with DAPI to show nuclei (in blue). The sorted ECs from the GBM xenografts do not contain any cell expressing the human cell-specific nuclear antigen NuMA.
- (L) Quantification of the fractions of the human GBM cell- or mouse-derived pericytes and ECs in the freshly sorted pericyte population and EC population from the GBM xenografts. More than 70% of the freshly sorted pericytes (CD146+CD248+) from GBM xenografts are positive for the human cell-specific antigens NuMA, whereas the freshly sorted ECs (CD31*CD105*) from the same xenografts are completely negative for the human cell-specific antigen NuMA, indicating that ECs are mouse-derived and rarely derived from human cancer cell in the GBM xenografts.

All scale bars represent 25 μm . The error bars represent SD.

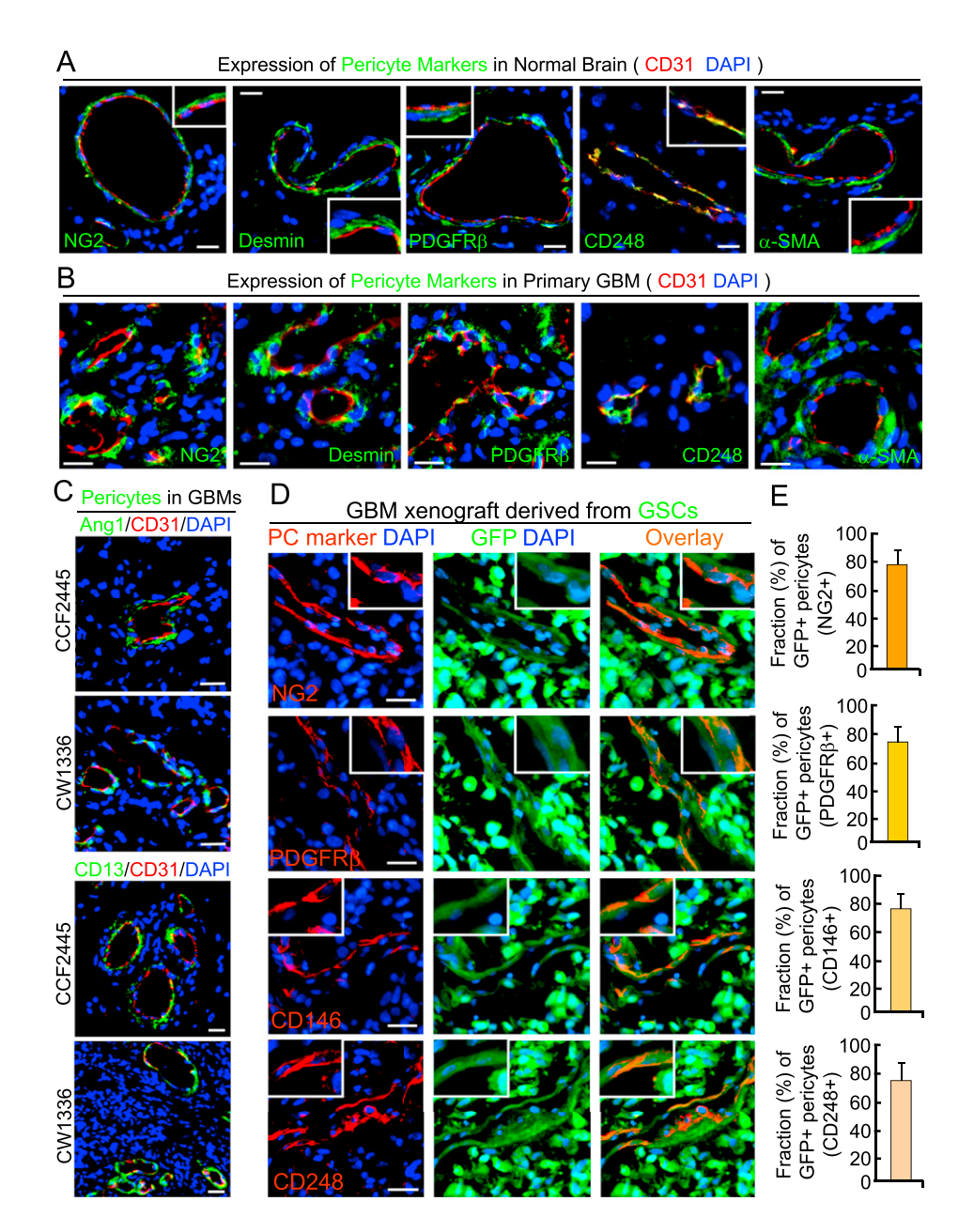


Figure S2. G-Pericytes in Xenografts Express Similar Pericyte Markers as Vascular Pericytes in Normal Brain and Primary GBMs, Related to Figure 2

(A) IF staining of pericyte markers (NG2, Desmin, PDGFRβ, CD248 and α-SMA) in normal brain. Frozen sections of normal brain tissue adjacent to a GBM tumor were immunostained with anti-CD31 antibody to mark ECs (in red) and a specific antibody against one of the pericyte markers (in green). Sections were counterstained with DAPI to mark nuclei (in blue). A portion of the vessel in each panel was enlarged and displayed at corner of the picture. Vascular pericytes in normal brain tissue show abundant expression of the pericyte markers.

(B and C) IF staining of pericyte markers (NG2, Desmin, α-SMA, PDGFRβ, CD248, Ang1 and CD13) in primary GBM tumors. Frozen sections of primary GBMs (B: CCF2509; C: CCF2445 and CW1336) were immunostained with anti-CD31 antibody to mark ECs (in red) and a specific antibody against one of the pericyte markers (in green). Sections were counterstained with DAPI to mark nuclei (in blue). Although pericytes surrounding the tumor vessels appear abnormal, these tumor pericytes also express the specific pericyte markers that are expressed by pericytes in normal brain.

(D and E) In vivo cell lineage tracing of GSCs with GFP constitutive expression and IF staining of pericyte markers in the GSC-derived GBM xenografts. GSCs from a primary GBM (CW738) were transduced with GFP stable expression and then transplanted into mouse brains to establish GBM xenografts. Frozen sections of the GBM xenografts were immunostained with specific antibodies against the pericyte markers (NG2, CD146, PDGFR β or CD248, in red) and counterstained with DAPI to show nuclei (in blue). Representative images of tumor vessels with GFP+ pericytes expressing NG2, PDGFRβ, CD146 or CD248 are shown in (D). Quantifications (E) shows that the majority (>78%) of the pericyte marker-expressing cells are GFP positive (in green), confirming that GSCs generate the majority of vascular pericytes in the GBM xenografts.

All scale bars represent 25 $\mu m.$ The error bars represent SD.

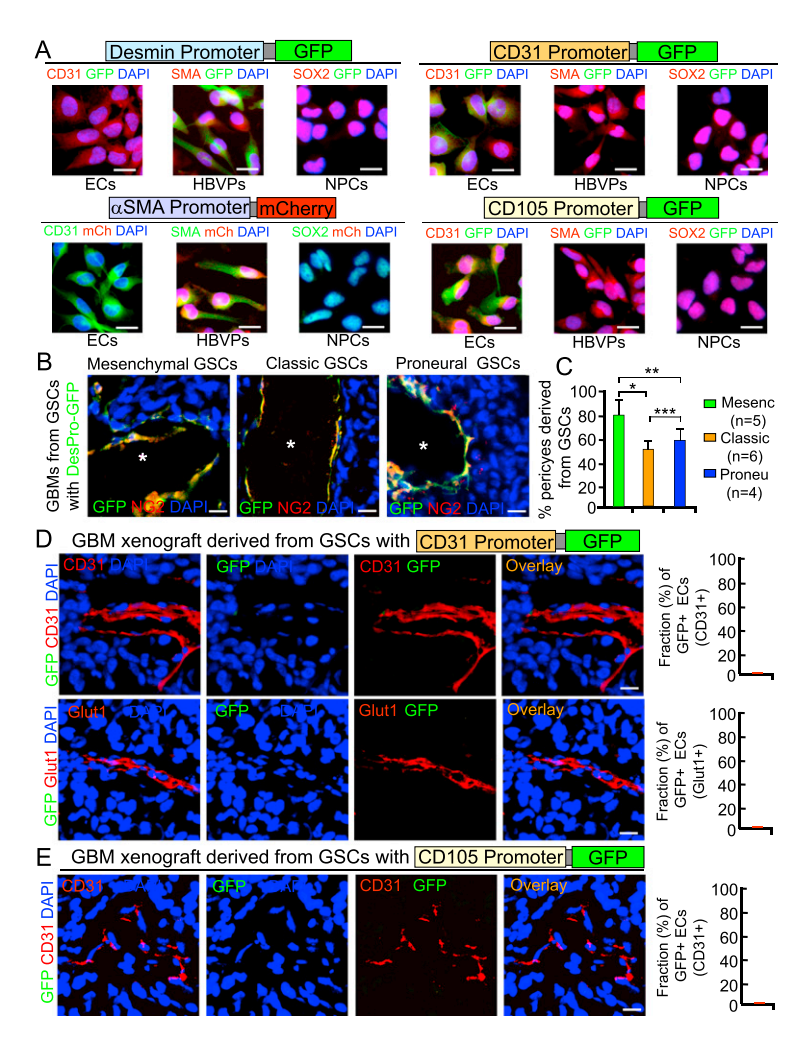


Figure S3. In Vivo Cell Lineage Tracing of GSCs with Pericyte or EC-Specific Promoter-Driven Fluorescent Reporters, Related to Figure 3

(A) Cell type-specific expression of the Desmin promoter-driven GFP, α -SMA promoter-driven mCherry, CD31 or CD105 promoter-driven GFP constructs in the in vitro functional test. Endothelial cells (HBMECs), pericytes (HBVPs) and neural progenitor cells (NPCs) were transduced with the indicated expression constructs through lentiviral infection, and then immunostained with a specific antibody against a cell type marker (CD31 for ECs, α-SMA for pericytes, and SOX2 for NPCs). Nuclei were counterstained with DAPI (in blue). The Desmin promoter-driven GFP expression (green) or α-SMA promoter-driven mCherry (in red) was detected in pericytes, but not in ECs and NPCs (left panels), whereas the CD31 or CD105 promoter-driven GFP expression (green) was detected in ECs, but not in pericytes and NPCs (right panels), validating that the reporter expression systems controlled by the lineage-specific promoters are functional and cell typespecific.

(B and C) In vivo cell lineage tracing of GSCs with different TCGA subtype by using the Desmin promoter-driven GFP expression in the xenografts. The TCGA subtypes of GBMs were determined by RT-PCR analysis of molecular signature of EGFR, PTEN, NF1, IDH1 and PDGFRα in the tumor cells (Table S1). Mesenchymal GBMs: EGFR wild-type and PTEN or NF1 deletion/mutations; Classic GBMs: EGFR amplification or expression of EGFR^{vill}; Proneural/neural GBMs: PDGFRa amplification but EGFR wild-type. The GSCs isolated from primary GBMs with mesenchymal, classic or proneural subtype were transduced with DesPro-GFP through lentiviral infection and then transplanted into mouse brains to establish GBM xenografts. Frozen sections of the GBM xenografts were immunostained with the specific antibody against the pericyte marker (NG2, in red) and counterstained with DAPI to show nuclei (in blue). Quantification (C) shows that the fraction (%) of the G-pericytes in the GBM xenografts derived from mesenchymal GSCs is significantly higher than that in the GBM xenografts derived from classic or proneural GSCs, indicating that mesenchymal GSCs have significantly greater ability to generate vascular pericytes than classic and proneural GSCs in vivo. *p < 0.002; **p < 0.003; ***p > 0.5.

(D) In vivo cell lineage tracing of GSCs with the CD31 promoter-driven GFP in GBM xenografts. The freshly sorted GSCs (CW777) were transduced with CD31 Pro-GFP and transplanted into mouse brains to establish GBM xenografts. Tumor sections from the GBM tumors were immunostained with the specific antibody against CD31 or Glut1 (EC markers, in red) and counterstained with DAPI to show nuclei (in blue). No GFP-positive EC was detectable in the GBM xenografts, indicating that GSCs did not give rise to ECs in vivo.

(E) In vivo cell lineage tracing of GSCs with CD105 promoter-driven GFP in GBM xenografts. The freshly sorted GSCs from a primary GBM (CCF2049) were transduced with CD105Pro-GFP and then transplanted into mouse brains to establish GBM xenografts. Frozen sections of the GBM xenografts were immunostained with the anti-CD31 (in red) and counterstained with DAPI (in blue). No GFP+ EC was detectable in the GBM xenografts, confirming that GSCs did not generate ECs in vivo.

The scale bars represent 10 μm (A) and 25 μm (B, D and E). The error bars represent SD.

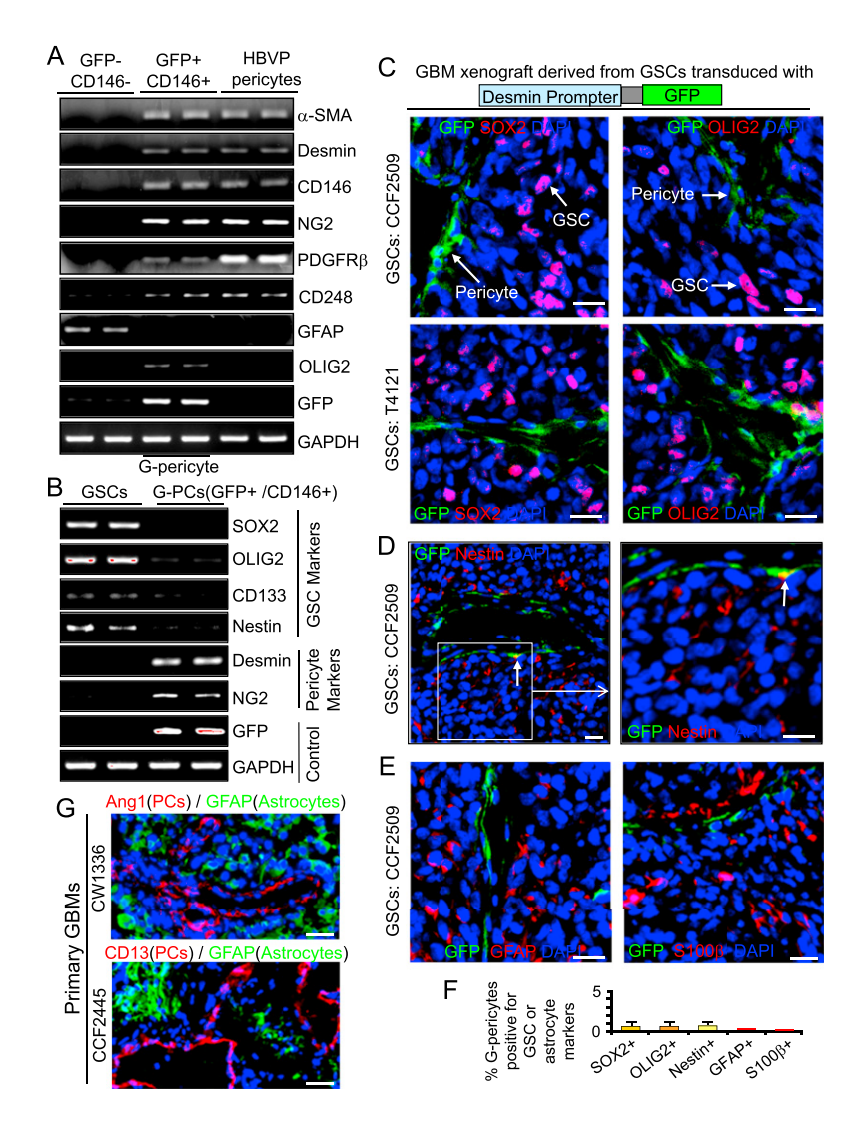


Figure S4. G-Pericytes Express Similar Pericyte Markers as Normal Brain Vascular Pericytes but Rarely Express GSC or Astrocyte Markers, **Related to Figure 3**

(A) RT-PCR analysis of pericyte marker expression in G-pericytes and human brain vascular pericytes (HBVPs). G-pericytes were obtained by sorting GFP+CD146+ cells from the xenografts derived from the DesPro-GFP GSCs. GFP-CD146- cells sorted from the same xenografts were used for negative control. Normal vascular pericytes (HBVP line, from ScienCell) were used for positive control. RNA samples isolated from these cells were subjected to RT-PCR analyses to examine the expression of several pericyte markers (α-SMA, Desmin, CD146, NG2, PDGFRβ and CD248), an astrocyte marker (GFAP) and a GSC marker (OLIG2) in these cells. GFP serves as a positive marker for the G-pericytes isolated from the DesPro-GFP GSC xenografts. G-pericytes and HBVP pericytes show similar, but not identical, expression of the pericyte markers.

(B) RT-PCR analysis of GSC marker expression and pericyte marker expression in GSCs and G-pericytes. The G-pericytes (GFP*CD146*) were isolated from DesPro-GFP GSC xenografts. The freshly sorted G-pericytes barely express the NSC or GSC markers (SOX2, OLIG2, CD133 and Nestin), whereas the GSCs do not express the pericyte markers (Desmin and NG2). The expression of GFP in the sorted G-pericytes (GFP+CD146+) serves as a positive control for this population.

(C-F) IF staining of GSC markers (SOX2, OLIG2 or Nestin, in red) and astrocyte markers (GFAP or S100β, in red) on tumor sections of GBM xenografts derived from the DesPro-GFP-transduced GSCs. The GSCs from a primary GBM (CCF2509) or a GBM xenograft (T4121) were transduced with the Desmin promoterdriven GFP through lentiviral infection, and then transplanted into mouse brain to establish GBM xenografts. Frozen sections of the xenografts were immunostained with the specific antibody against SOX2, OLIG2, Nestin, GFAP or S100β (in red), and counterstained with DAPI to show nuclei (in blue). The G-pericytes (GFP+, in green) rarely express the GSC marker SOX2, OLIG2 or Nestin, while GSCs expressing SOX2, OLIG2 or Nestin (in red) are distributed in the perivascular niches but rarely overlap with GFP+ cells (G-pericytes) in the GBM xenografts (C and D). G-pericytes (GFP+) do not express any astrocyte marker GFAP or S100β (in red) (E). Quantification (F) shows that a small fraction (0.9%-1.6%) of G-pericytes (GFP+) are positive for the GSC markers (SOX2, OLIG2 or Nestin) but no Gpericyte showed positive for the astrocyte markers.

(G) IF staining of the astrocyte marker (GFAP) and the pericyte markers (Ang1 and CD13) in primary GBMs. Frozen sections of GBMs (CCF2445 and CW1336) were immunostained with specific antibodies against GFAP (in green) and Ang1 or CD13 (in red), and then counterstained with DAPI to show nuclei (in blue). Pericytes and astrocytes are two distinct populations without overlapping expression of their markers in the primary GBMs. All scale bars represent 25 µm.

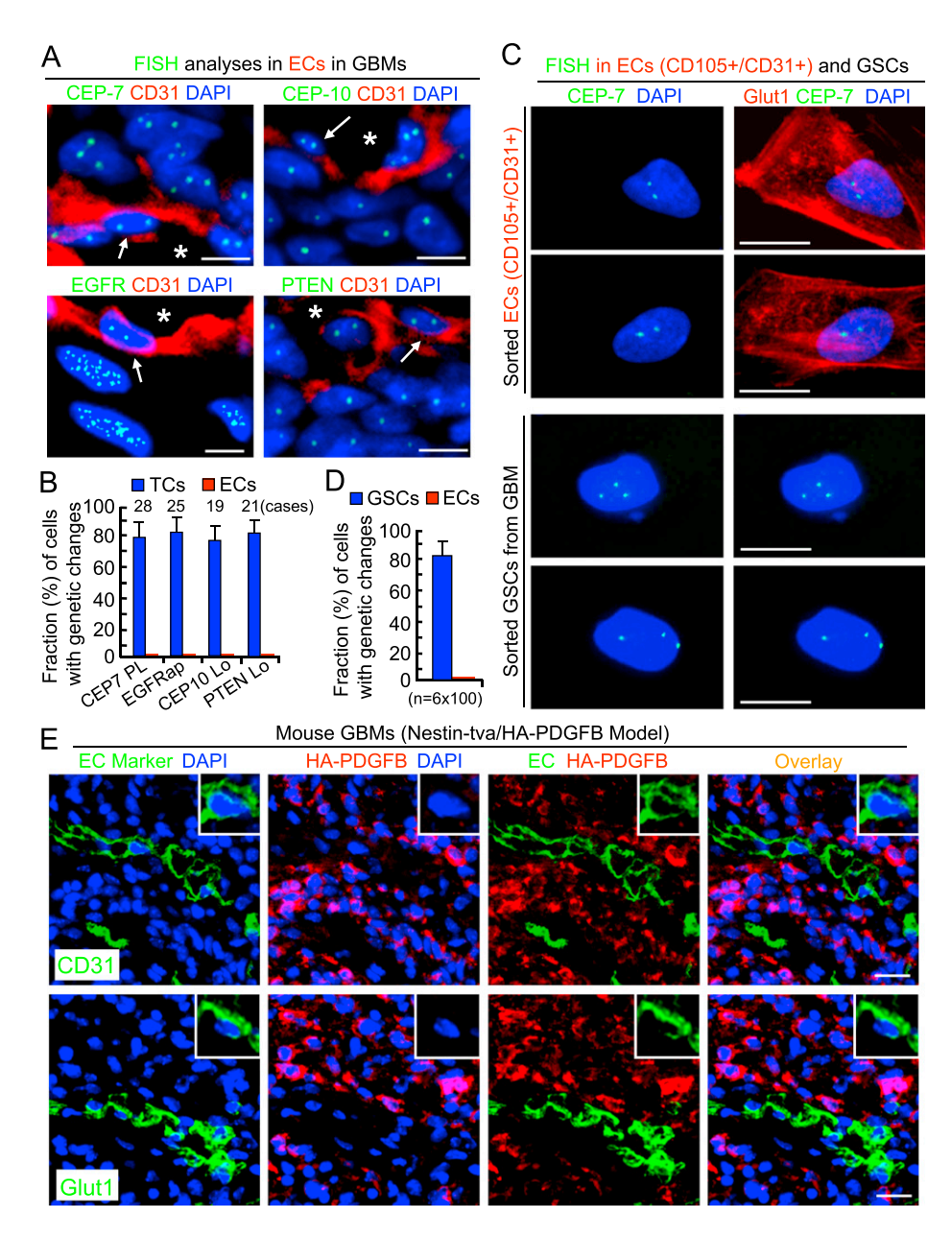


Figure S5. Endothelial Cells Are Rarely Derived from Cancer Cells in Human Primary GBMs and the Genetically Engineered Mouse GBMs, Related to Figure 4

(A) Fluorescence in situ hybridization (FISH) analyses of genetic alterations with FITC-conjugated probes of CEP-7, CEP-10, EGFR and PTEN (in green) in vascular ECs marked by CD31 staining (in red) and in cancer cells in primary GBMs. Representative images of ECs positive for CD31 are indicated by white arrows. ECs did not carry the same genetic alterations as cancer cells. * marks the vessel lumen.

(B) Quantification shows that tumor ECs rarely carry the cancer genetic alterations (CEP-7 polysomy, 28 cases; EGFR trisomy or amplification, 25 cases; CEP-10 loss, 19 cases; or PTEN loss, 21 cases) in 56 cases of primary GBMs in tissue arrays. TCs: tumor cells; ECs: Endothelial cells.

(C and D) FISH analysis with CEP-7 probe in the freshly sorted ECs and GSCs from primary GBMs. The sorted ECs (CD31+CD105+) and GSCs were subjected to FISH analysis with FITC-conjugated CEP-7 probe (in green) and IF staining of Glut1 (another EC marker, in red), and counterstained with DAPI to show nuclei (in blue). Representative images of FISH analysis with CEP-7 (in green) and Glut1 staining (in red) in sorted ECs and GSCs from a primary GBM (CW837) are shown in (C). Quantification (D) shows that the sorted ECs from six primary GBMs rarely carry the same genetic alterations (CEP-7 polysomy or CEP-10 loss) as GSCs. (E) IF staining of EC markers in the genetically engineered mouse GBMs (Nestin-tva/Ink4a/Arf^{-/-}/HA-PDGFB models). Frozen sections of the mouse GBM tumors were immunostained with specific antibodies against EC markers (CD31 or Glut1, in green) and HA-tag to detect cancer cells expressing HA-PDGFB (in red), and then counterstained with DAPI to show nuclei (in blue). Typical cells showing positive for the EC marker are enlarged and displayed at corners of the panels. Vascular ECs in the mouse GBMs do not express HA-PDGFB (cancer cell marker in this tumor model), indicating ECs are rarely derived from the cancer cells. The scale bars represent 10 μm (A and C) and 25 μm (E). The error bars represent SD.

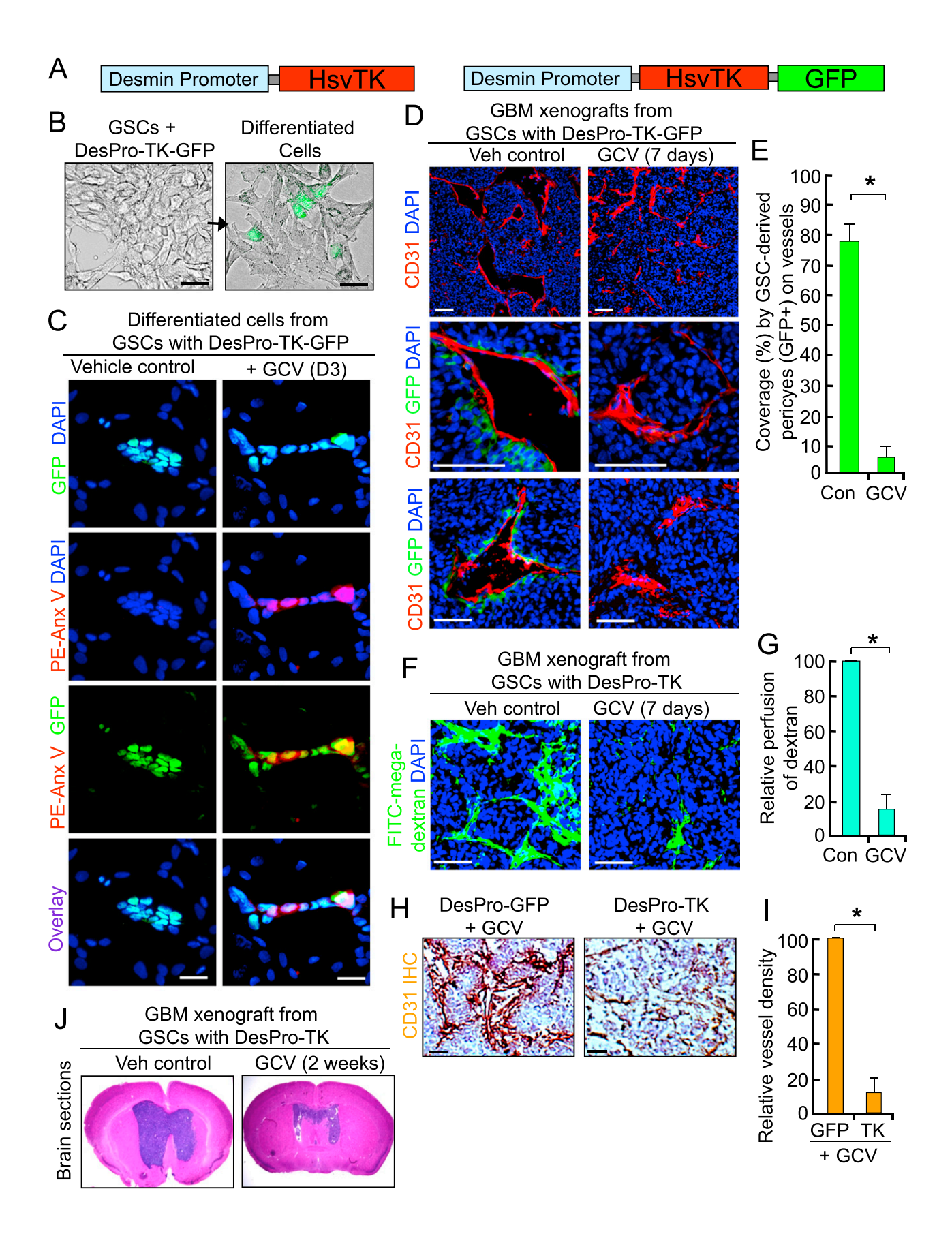


Figure S6. Selective Targeting of G-Pericytes Disrupts Vascular Structure and Function in GBM Xenografts, Related to Figure 5

(A) Schematic illustrations of lentiviral constructs for the Desmin promoter-driven expression of HsvTK (herpes simplex virus thymidine kinase) or coexpression of HsvTK and GFP (DesPro-TK or DesPro-TK-GFP). Desmin promoter (312 bp) with an enhancer (284 bp) was cloned from human genomic DNA. The Desmin promoter-driven expression of HsvTK or/and GFP should occur specifically in G-pericytes after GSCs are transduced with the construct.

(B) In vitro cell lineage tracing of GSCs with Desmin promoter-driven GFP expression. The isolated GSCs (CCF2045) were transduced with DesPro-TK-GFP through lentiviral infection, and then induced to differentiate. The expression of GFP was turned on in some of differentiated cells derived from the GSCs transduced with DesPro-TK-GFP (right panel).

(C) Detection of apoptotic cells by the PE-conjugated anti-Annexin V antibody (PE-Anx V) in differentiated cells derived from the DesPro-TK-GFP transduced GSCs after GCV treatment. GSCs were transduced with DesPro-TK-GFP through lentiviral infection and then induced to differentiate in DMEM with 10% FBS. The differentiated cells were treated with GCV or vehicle control for 48 hr and then immunostained with PE-conjugated anti-Annexin V antibody (in red) to detect apoptotic cells. Nuclei were counterstained with DAPI (blue). GCV treatment selectively induced apoptosis in the G-pericytes (GFP+).

(D and E) IF staining of CD31 showing effects of selective targeting of G-pericytes on vessel structure in GBM xenografts. GSCs (D456) were transduced with DesPro-TK-GFP through lentiviral infection, and then transplanted into mouse brains to establish GBM xenografts. Mice bearing the GBM tumors were treated with ganciclovir (GCV) or vehicle control daily for 1 week. Frozen sections from the GBM tumors were immunostained with anti-CD31 antibody to mark ECs (in red) and analyzed for G-pericytes (GFP+, in green). GCV treatment resulted in depletion of G-pericytes (loss of GFP+ cells surrounding the vessels), closure of vessel lumens and disruption of vascular walls in GBM xenografts (right panels). Quantification (E) shows that GCV treatment significantly reduced vessel pericyte coverage by the GSC-derived pericytes (GFP+). *p < 0.001.

(F and G) Assessment of vascular function with FITC-conjugated mega-dextran (in green) in the GBM xenografts after selective elimination of G-pericytes by GCV treatment. Mice bearing the GBM tumors derived from Des-TK-transduced GSCs were treated with GCV or vehicle control for 1 week, perfused with FITC-megadextran for 60 min, and then harvested for fluorescent analysis of FITC-mega-dextran perfusion in tumors. Frozen sections of the GBM xenografts were counterstained with DAPI (blue) and then examined for intensity of perfused FITC-mega-dextran. Quantification (G) shows that selective elimination of G-pericytes by GCV treatment significantly reduced FITC-mega-dextran perfusion into tumors. *p < 0.001.

(H and I) Immunohistochemical (IHC) staining of CD31 to examine vessel density in GBM xenografts after selective elimination of G-pericytes by GCV treatment. Mice bearing the GBM tumors derived from GSCs (CCF2170) transduced with DesPro-TK or DesPro-GFP (control) were treated with GCV for 2 weeks, and the tumor sections were analyzed by IHC staining of CD31 to mark blood vessels. Sections were counterstained with hematoxylin for nuclei. GCV treatment disrupted vessels in the GBM tumors derived from GSCs transduced with DesPro-TK, but not in control tumors derived from GSCs transduced with DesPro-GFP. Quantification (I) shows that selective targeting of G-pericytes by GCV treatment significantly reduced vessel density in GBM xenografts derived from GSCs with DesPro-TK, but not in the control xenografts derived from GSCs with DesPro-GFP. *p < 0.001.

(J) Representative images of cross sections (H&E stained) of mouse brains bearing the GBM xenografts derived from GSCs transduced with Desmin promoterdriven TK after GCV or vehicle control treatment for 2 weeks. GSCs (CCF2170) were transduced with DesPro-TK and then transplanted into mouse brains to establish GBM xenografts. Mice bearing the GBM tumors were treated with ganciclovir (GCV) or vehicle control daily for 2 weeks. Cross sections of mouse brains bearing the GBM xenografts were analyzed by H&E staining. GCV treatment depleting the G-pericytes expressing HsvTK potently inhibited tumor growth of GBM xenografts derived from GSCs with DesPro-HsvTK.

The scale bars represent 25 µm (B and C) and 100 µm (D, F and H). The error bars represent SD.

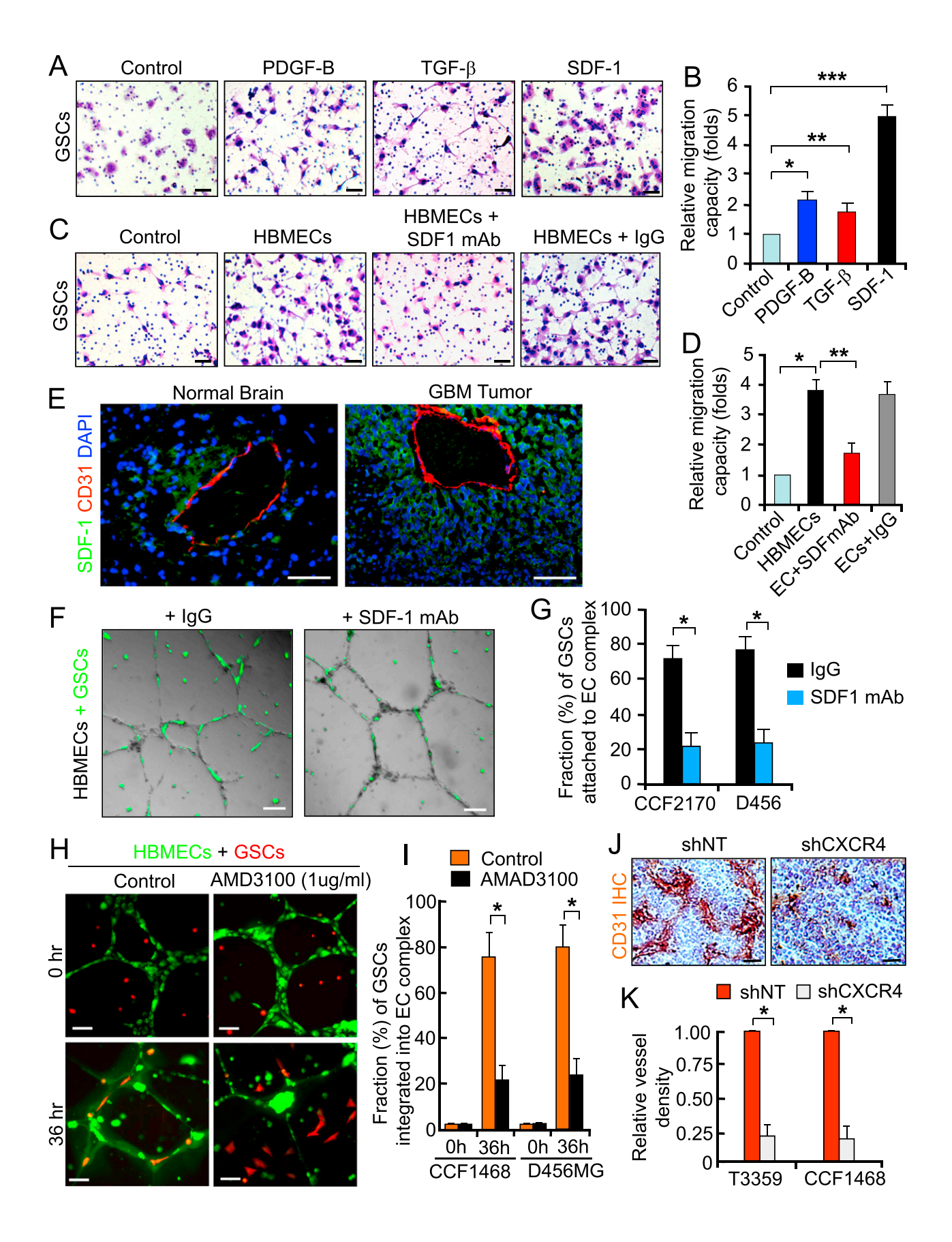


Figure S7. Glioblastoma Stem Cells Are Recruited toward Endothelial Cells via the SDF-1/CXCR4 Axis to Generate Vascular Pericytes, Related to Figure 6

(A and B) In vitro matrigel invasion assay showing that SDF-1α (CXCL12) is a dominant cytokine to attract GSC migration. GSCs (CW619) were added to upper chambers and the cytokines were added to lower chambers of the transwells in the matrigel invasion assay. Cells migrated through the matrigel were stained and the representative images are shown in (A). Quantification (B) indicates that SDF-1 potently promotes GSC migration through the matrigel. *p < 0.04; **p < 0.09; ***p < 0.001.

(C and D) In vitro matrigel invasion assay showing that HBMECs attract GSC toward the ECs and this effect was attenuated by the SDF-1 blocking antibody. GSCs (CW702) were added to upper chamber and HBMECs were cultured on bottom chamber without or with SDF-1 blocking antibody (SDF1 mAb) or IgG control in the Boydern chambers. GSCs migrated through the matrigel were stained and representative images from the indicated conditions are shown in (C). Quantification (D) shows that HBMECs promote GSC migration through the matrigel, and this effect was significantly inhibited by the SDF-1 blocking antibody (D). *p < 0.001; **p < 0.002.

(E) IF staining of SDF-1 (in green) and CD31 (in red) in normal brain tissue and a primary GBM tumor. Sections of a human primary GBM tumor (CCF2045) and the adjacent normal brain tissue were immunostained with specific antibodies against SDF-1 (in green) and the EC marker CD31 (in red). Nuclei were counterstained with DAPI (blue). Blood vessels in both brain tissue and GBM tumor produce abundant SDF-1 that forms chemo-attractant gradient around the vessels.

(F and G) In vitro endothelial complex formation assay showing that recruitment of GSCs toward HBMEC complex was inhibited by the SDF-1 blocking antibody. GFP-labeled GSCs (CCF2170) were added to the established HBMEC complex in the presence of the anti-SDF-1 mAb or IgG control. The integration of GSCderived cells (in green) into the endothelial complex was monitored. The representative merged images of HBMEC complex with GSC-derived cells at 36 hr after cell mixing are shown (F). Quantification (G) shows the fractions of GSC-derived cells (GFP+) integrated into the EC complex in the presence of SDF-1 mAb or IgG at 36 hr. The SDF-1 blocking antibody significantly inhibited the recruitment of GSCs (D456 and CCF2170) to the endothelial complex. *p < 0.001.

(H and I) The Effect of CXCR4 inhibition by AMD3100 on recruitment and integration of GSCs to HBMEC complex. HBMECs labeled with the green fluorescent cell tracer CFSE were allowed to form endothelial complexes (in green). The GSCs (D456MG or CCF1468) labeled with the red fluorescent cell tracer CMTRX (in red) were added to the HBMEC complex in the presence of AMD3100 or vehicle control. The representative images of the EC complex at indicated time points are shown (H). Quantification (I) shows the fractions of GSC-derived cells integrated into HBMEC complex in the presence of AMD3100 or vehicle control at indicated time points. AMD3100 significant inhibited the recruitment and integration of GSC-derived cells into HBMEC complex. *p < 0.001.

(J and K) Immunohistochemical (IHC) staining of CD31 to examine the effect of CXCR4 knockdown in GSCs on vessel density in the GBM xenografts. Tumor sections from the GBM xenografts derived from GSCs expressing nontargeting shRNA (shNT) or CXCR4 shRNA (shCXCR4) were analyzed by IHC staining of CD31 (in brown). Representative images of the vascular staining in the GBM tumors are shown in (J). Quantification (K) shows that the vessel density was significantly reduced in GBM xenografts derived from GSCs expressing shCXCR4 relative to control xenografts derived from GSCs expressing NT shRNA.*p <

The scale bars represent 25 μm (A and C) and 100 μm (E, F, H and J). The error bars represent SD.